11-16-2011

The Reactive Carbonyl Methylglyoxal Suppresses Vascular KATP Channels by MRNA Destabilization

Anuhya S. Konduru

THE REACTIVE CARBONYL METHYLGLYOXAL SUPPRESSES VASCULAR K_{ATP} CHANNELS BY MRNA DESTABILIZATION

by

ANUHYA SHARMA KONDURU

Under the guidance of Dr. Chun Jiang

ABSTRACT

Diabetes mellitus is characterized by hyperglycemia, oxidative stress and excessive production of intermediary metabolites including methylglyoxal (MGO), a reactive carbonyl. MGO can readily interact with proteins, lipids and DNA, and cause an imbalance of the cellular antioxidant system leading to carbonyl stress. The effects of MGO can be devastating if the targeted molecules are responsible for the maintenance of membrane potentials and ionic homeostasis. Here we show that MGO disrupts the vascular isoform of ATP-sensitive K^+ (K_{ATP}) channels by acting on the mRNAs of Kir6.1 and SUR2B subunits thereby regulating vascular tone. Our results show that the 3' untranslated region (UTR) of Kir6.1 mRNA and the coding region of SUR2B mRNA are targeted by MGO causing a disruption of vascular K_{ATP} channels. The destabilization of the mRNAs of K_{ATP} channel can in turn affect K^+ homeostasis of vascular smooth muscles as well as vascular responses to circulating vasodilators and vasoconstrictors.

INDEX WORDS: Kir6.1, SUR2B, Hyperglycemia, Methylglyoxal, MGO, Reactive carbonyl species, Carbonyl stress, Vascular tone, Potassium channels, Untranslated region, Coding region, MRNA stability.

THE REACTIVE CARBONYL METHYLGLYOXAL SUPPRESSES VASCULAR K_{ATP} CHANNELS BY MRNA DESTABILIZATION

by

ANUHYA SHARMA KONDURU

A Thesis Submitted in Partial Fulfillment of the Requirements for the Degree of

Master of Science

In the College of Arts and Sciences

Georgia State University

2011

THE REACTIVE CARBONYL METHYLGLYOXAL SUPPRESSES VASCULAR K_{ATP} CHANNELS BY MRNA DESTABILIZATION

Committee chair: Dr.Chun Jiang

Committee: Dr. Andrew Clancy

Dr. Ritu Aneja

Electronic Version Approved:

Office of Graduate Studies

College of Arts and Sciences

Georgia State University

December 2011

ACKNOWLEDGEMENTS

First and foremost I would like to thank my advisor Dr. Chun Jiang, for his support and encouragement motivates me to deliver my best on the scientific front. It has been an honor and pleasure to be associated with Jiang lab for the last eighteen months. I am also grateful to my committee member Dr. Andrew Clancy and Dr. Ritu Aneja, whose valuable suggestions and advice has helped me to conduct better science and shape by study better.

I am indebted to all the past and current members of Jiang lab, for enriching my personal and professional experience during my stay in the lab. I owe my deepest gratitude to Dr. Yang Yang (an alumnus of Jiang lab) for mentoring me right from my initial days in research environment and seeing me through till the completion of my thesis. Dr. Yang continues to support me in all my career related issues and has a great influence on shaping my attitude and thoughts towards science and research. I would like to thank Mr. Timothy Trower (student research assistant) for his suggestions and assistance with experiments, that have helped me trouble shoot many experiment related issues. Mr. Trower is also an amazing friend, who was always around during my slog periods and helped me pull myself back on track many a times.

I would like to give a special mention to Ms. LaTesha Warren, for she always had my back for all the administrative issues at all times during the period of my graduate study at Georgia State. I am grateful to Mr. Charles Bush, Supply Manager – NSC stock room for always accommodating my requests for chemicals and reagents, even within short periods of notice.

No words are enough to express my gratitude to my mother Mrs. Deepika Konduru and brother Mr. Anmol Konduru (Potter) for their prayers and moral support. My dearest friends Ms. Priya and Ms. Abby deserve bountiful love for their care and support during all my endeavors.

TABLE OF CONTENTS

LIST OF FIGURES

LIST OF TABLES

ABBREVIATIONS

A-10	vascular smooth muscle cells
AGE	advanced glycation endproduct
ANOVA	analysis of variance
ATP	adenosine triphosphate
cAMP	cyclic adenosine monophosphate
DAG	diacylglycerol
DMEM	Dulbecco's Modified Eagle Medium
DMSO	dimethyl sulfoxide
EC	endothelial cell
GAPDH	glyceraldehyde 3-phosphate dehydrogenase
GSH	reduced glutathione
HEK	human embryonic kidney cells
hRluc-neo	renilla luciferase gene
IC_{50}	concentration for 50% inhibition
K_{ATP}	ATP-sensitive K^+
Kir	inward rectifier K^+ channel

luc2	firefly luciferase gene
MGO	methylglyoxal
mRNA	messenger RNA
PCR	polymerase chain reaction
PKC	protein kinase C
pmirGLO	Dual Glo luciferase vector
qPCR	quantitative real-time PCR
RAGE	receptor for advanced glycation endproduct
RCS	reactive carbonyl species
S.E.	Standard error
SUR	sulphonylurea receptor
VDCC	voltage-dependent Ca^{2+} channel
VSM	vascular smooth muscle
VSMC	vascular smooth muscle cell
UTR	untranslated regio

1. INTRODUCTION

1.1 Reactive carbonyl species

Carbonyl species are compounds containing the (C=O) carbonyl functional group. As oxygen atom in the carbonyl group is more electronegative than the carbon atom, it pulls the electrons from the carbon atom and thereby increases the polarity of the carbonyl group. The carbonyl carbon is electrophilic in nature and readily reacts with nucleophiles. The carbonyls methylglyoxal (MGO), glyoxal, acrolein, hydroxyhexenal, hydroxynonenal (HNE) are highly reactive compared to other carbonyls produced in the biological system (Ellis, 2007). These carbonyls are collectively called reactive carbonyl species (RCS). RCS are more stable than the free radicals, and can diffuse over long distances to reach its target molecules (Lesgards et al., 2011).

1.2 Carbonyls in pathological conditions

Diabetes mellitus is a systemic disorder that affects 8.3% of the population in the United States (Department of Health and Human Services, 2011). Persistent hyperglycemia in diabetic patients causes metabolic alterations, leading to overproduction of a variety of intermediary metabolites. One of the metabolites is the reactive α,β-dicarbonyl, MGO which is both an aldehyde and a ketone. MGO has been attributed to be responsible for the development and progression of diabetes and diabetes associated vascular complications (Bourajjaj et al., 2003) like atherosclerosis, ischaemia, hypertension, retinopathy and nephropathy (Brownlee, 2001). All of the diabetes associated vascular complications are characterized by a variety of changes in the micro and macro vasculatures. Most of these changes are due the impairment of the appropriate response of the vasculatures to vascoactive substances, hormones, neurotransmitters, cytokines

etc. The changes in the vasculature can be one of the following or a consortium of many. Abnormal function of the vasculature and high potential for thrombosis can lead to atherosclerosis. Inflammation, presence of high levels of oxidants and stiffening of the vasculature and improper expression of surface markers are also markers for vascular complications (Creager et al., 2003). In Alzheimer's disease an increase in the levels of acrolein, HNE and acrolein modified proteins have been identified (Lovell et al., 2001). Increased levels of HNE and HNE modified proteins have also been identified in hypertension (Asselin et al., 2006). HNE has also been identified in atherosclerotic plaques (Leonarduzzi et al., 2005). MGO is also thought to be present in the amyloid plaques (Kuhla et al., 2005).

1.3 Production of MGO

MGO is produced via both enzymatic and non-enzymatic reactions. MGO is mainly produced via glucose metabolism, through the transformation of triosephosphate intermediates – glyceraldehyde-3-phosphate (GAPDH) and dihydroxy acetone phosphate (DHAP) (Cooper, 1984; Pompliano et al., 1990; Thornalley, 1990) by methylglyoxal synthase. MGO is also formed by the metabolism of aminoacetone or acetone from lipolysis, which is catalyzed by semicarbazide-sensitive amine oxidase (SSAO) and acetol monooxygenase (Casazza et al., 1984; Lyles and Chalmers, 1992). This conversion can also happen via a non-enzymatic reaction in which aminoacetone is converted to MGO in the presence of Fe^{+2} as catalyst (Dutra et al., 2001). Additionally MGO is also formed during the cellular metabolic process like protein metabolism (Lyles and Chalmers, 1992). Proteins containing L-threonine undergo oxidation in the mitochondria to form glycine and acetyl-CoA via the intermediate 2-amino-3-oxobutyrate (Bird et al., 1984). In case of diabetes, 2-amino-3-oxobutyrate is driven towards formation of aminoacetone, a precursor for MGO production (Kalapos, 2008).

All forms of diabetes are associated with hyperglycemia and increase in the levels of reactive oxygen species (ROS) like superoxide anion (O_2^-), hydroxyl ion (OH^-), and non-radical reactive species like hydrogen peroxide (H_2O_2). Increased levels of intracellular oxidants can lead to the peroxidation of membrane lipids (Esterbauer et al., 1991), which can lead to the generation of carbonyl species like MGO, through a series of oxidative and rearrangement reactions (Esterbauer et al., 1982). Reducing sugars can react with the amino groups of Lys and Arg residues on proteins to form Schiff's bases via a Maillard reaction. The Schiff bases can undergo a series of rearrangement reactions to form advanced glycation end products (AGEs) (Thornalley et al., 1999). Oxidation of the thus formed AGEs leads to the generation of carbonyl species like MGO, glyoxal, acrolein (Thornalley, 2005). Under hyperglycemic conditions increased flux through the polyol - fructose pathway is observed which leads to the formation of MGO (Desai et al., 2010).

1.4 Reactivity of MGO

MGO is highly reactive due to the presence of the ketone group at C2 in addition to the aldehyde group at C1. The carbonyl groups are electrophilic and can undergo addition with the nucleophilic groups on proteins, DNA, RNA and lipids (Cooper et al., 1987; Marnett et al., 1985).

1.4.1 Protein modification by MGO

The carbonyl groups (aldehyde/ketone) of MGO can react with the amino group (NH_4^+) on the amino acids Lys and Arg to form Schiff bases (compounds containing C=N), the formation of which are reversible. The Schiff bases can undergo a series of acid or base catalyzed isomerization reactions that lead to the formation of Amadori products (rearranged Schiff's base in which the nitrogen in C=N is bound by a hydrogen atom from the adjacent OH^-).

The Amadori products can further undergo a series of condensation, oxidation in presence of metals and dehydration reactions to AGEs (Wautier and Schmidt, 2004). MGO reacts with the Arg and Lys residues on proteins to form the AGEs 5-hydro-5-methylimidazolones (Thornalley et al., 2003), argypyrimidine (Shipanova et al., 1997) and N^{ε}-carboxymethyl lysine, N^{ε}-carboxyethyl lysine (Ahmed et al., 2002) adducts respectively. Additionally the carbonyl groups of MGO can also react with the sulphydryl groups (-SH) on the Cys residues on proteins to form glycation adducts (Sato et al., 1980). The protein glycation adducts are stable and thus pose problems for the normal functioning of the biological system.

1.4.2 Modification of nucleotides by MGO

MGO preferentially reacts with the NH_2 groups present on the guanine nucleotides to form tricyclic compounds (Vaca et al., 1994). MGO reacts with the deoxyguanidine (dG) nucleotides to form 3-(2′-deoxyribosyl)-6,7-dihydro-6,7-dihydroxy-6-methylimidazo-[2,3-b]purine-9(8)one and N2-(1-carboxyethyl)-deoxyguanosine (Papoulis et al., 1995; Schneider et al., 1998). To differentiate from the MGO derived protein adducts, the MGO adducts formed with the nucleotides are called nucleotide AGEs.

MGO preferentially reacts with the single stranded nucleotides, RNA and denatured DNA. This is because the guanine nucleotides in native DNA molecules are protected from the electrophilic attack of MGO due to the double stranded structure (Krymkiewicz, 1973).

1.5 Metabolism of MGO

Irrespective of the production pathway, MGO is detoxified and maintained at normal levels in the cell by the glyoxalaseI/II system in presence of reduced glutathione (GSH). Glyoxalase I enzyme converts the MGO-GSH adducts into S-lactoylglutathione, following

which glyoxalase II enzyme converts S-lactoylglutathione into harmless D-lactate and releases the GSH (Chang and Wu, 2006) for the next round of detoxification.

In addition to the glyoxalase system, several other enzymes exist that facilitate the metabolism of MGO to other relatively harmless compounds. MGO contains two functional groups that can undergo either oxidation or reduction. MGO is also a substrate for the aldehyde dehydrogenase family of enzymes (ALDH2, ALDH3 and ALDH5), which can oxidize MGO into carboxylic acids (Vasiliou et al., 2004). This conversion also provides a protective role against oxidative stress (Ohsawa et al., 2003) in addition to carbonyl stress. Cytochrome P450 enzymes also facilitate the oxidation of the toxic aldehydes like MGO to carboxylic acids through hydroxylation of C-H bonds (Ellis, 2007). The enzymes aldehyde reductase (AKR 1A) and aldose reductase (AKR 1B) belonging to the family of aldo-keto reductases (AKR) play a role in reducing the aldehyde to alcohols, converting MGO to acetol and D-lactaldehyde (Vander Jagt et al., 1992). Alcohol dehydrogenase enzymes (ADH) are known to reduce the unsaturated double bond in the aldehydes to detoxify the aldehydes into alcohols (Hartley et al., 1995).

1.6 Carbonyl Stress

Under pathological conditions the levels of RCS exceed way above the normal levels as a consequence of the presence of increased amounts of the precursor molecules like plasma glucose, L-threonine, fructose, lipid peroxidation products and oxidants. Additionally in many pathological conditions the carbonyl detoxification system is impaired at the DNA or protein level (Thornalley, 2003). This leads to an accumulation of RCS, due to a failure in the clearance of RCS from the cell. This imbalance in the production and clearance of RCS leads to the phenomenon called carbonyl stress. Excess RCS are not only cytotoxic but can also act as mediators of oxidative stress and as secondary cytotoxic messengers (Lesgards et al., 2011).

Modification of proteins by RCS is more rapid compared to the modifications by its precursor glucose (Lo et al., 1994) even when present in low concentrations. MGO and MGO derived molecules have been identified as indicators of carbonyl stress in vivo (Baynes and Thorpe, 1999).

1.7 MGO toxicity

MGO can readily react with proteins and lipids leading to disruption of functional molecules and can cause structural damages to transporters, ion channels, transcription factors, signaling molecules and plasma membranes (Picklo et al., 2002). Double stranded DNA continuously opens up and closes throughout its structure thereby creating and closing gaps continously. MGO can bind to DNA at such gaps and can form DNA-MGO adducts (Krymkiewicz, 1973). These reactions proceed via reactions involving free radicals (Lo et al., 2006). The guanine residues on DNA and RNA can be targeted by MGO, which can lead to abnormalities in replication and transcription processes (Wu, 2006).

MGO reacts with the proteins to form AGEs/AGE precursor molecules (Thornalley et al., 1999). AGEs are involved in the pathogenesis associated with vascular complications related to many vascular diseases (Rosca et al., 2005). AGE precursors affect the target cells by several mechanisms. AGEs react with many intracellular proteins and alter the protein structure and function. AGE precursors can modify some of the extracellular matrix components, which can react abnormally with the receptors and structural components of the matrix on the cells. AGEs on extracellular matrix (ECM) interfere with the normal matrix-matrix and matrix-cell interactions. AGE induced crosslinks can alter the structure and function of the intact blood vessels by making them less elastic and more permeable (Brownlee, 2001). AGEs primarily target the structural components mainly collagen IV, fibrinogen, myelin, tubulin (Vlassara,

1996). Hydroimidazolone adducts formed by MGO can react with Type IV collagen in the vascular basement membrane and disrupt the integrin binding sites on the collagen (Vlassara, 1996). This leads to endothelial shedding and results in excess amounts of circulating endothelial cells (ECs). Increase in the circulating ECs is an indication of vascular damage associated with diabetes and uremia. MGO or AGE precursors can modify the plasma proteins in the cell to form AGEs. AGEs effect the cellular function by binding to specific receptors called receptors for advanced glycation end products (RAGE). RAGE are present on ECs, vascular smooth muscle cells (VSMCs), cardiac myocytes, macrophages and monocytes (Thornalley, 1998). Increased expression of RAGE on VSMCs and ECs has been observed in diabetes (Schmidt et al., 1999) . AGE receptor-ligand interaction induces ROS production and activates NF-κB transcription factor causing unwanted changes in the gene expression several cytokines and growth factors like TNF-α, TGF-β, GMCSF, pro-inflammatory molecules, cell adhesion molecules molecules like VCAM-1, that effects the cell-cell and cell-matrix communication (Brownlee, 2001). Glycated proteins are resistant to protein degradation mechanisms and can lead to the accumulation of AGEs in local environments (Brownlee, 1995). AGEs increase the levels of diacyl glycerol (DAG) which can activate different isoforms of PKC. Activated PKC has been shown to inhibit the K_{ATP} channel (Yang et al., 2008).

AGEs act on the –SH groups of antioxidant detoxifying enzymes like glyoxalase I (Thornalley, 2003) and superoxide dismutase (SOD) (Desai and Wu, 2008), glutathione reductase (Vander Jagt et al., 1997), to inactivate the enzymes. MGO can lower the levels of intracellular antioxidant - GSH leading to an imbalance in the oxidant-antioxidant ratio in the cells to cause oxidative stress (Thornalley, 2003). This leads to an overall decrease in the levels of functional antioxidant enzymes and leads to an impairment of the ROS and RCS clearance.

1.8 Carbonyl stress vs. Oxidative stress

MGO induced toxicity has been attributed to the presence of free radicals in both MGO generation and degradation processes (Kalapos, 2008). The enzymatic formation of methylglyoxal from aminoacetone yields H_2O_2, whereas a non-enzymatic conversion of aminoacetone to methylglyoxal releases O_2^-. Enzymatic conversion of acetol to methylglyoxal produces H_2O_2. Auto-oxidation and photolysis of MGO in the presence of OH^- has been reported to produce acetyl radicals (Nukaya et al., 1993). The ROS produced during MGO production can contribute to initiate or elevate cellular oxidative stress in the absence of appropriate detoxification systems. Oxidative stress is known to be associated with many cardiovascular diseases like diabetes, atherosclerosis, ischaemia, hypertension, aging, retinopathy, Alzheimers, end stage renal failure, inflammation (Ellis, 2007). In addition, oxidative stress can also lead to the production of several reactive aldehydes and ketones and thus contribute to carbonyl stress. Indeed, recent studies have shown that reactive carbonyls, rather than the initial ROS, are responsible for diabetic vascular complications (Ellis, 2007). Thus the relation between the generation of RCS and ROS is intertwined. The production of one kind of reactive species can lead to the generation of the other.

1.9 Maintenance of the vascular tone

Vascular tone is regulated by the combined action of several neuronal, hormonal mechanisms in addition to the local metabolic state of the cells to maintain homeostasis. Disruption of this regulation leads to cellular dysfunction and leads to the progression of severe diseases including diabetes associated macrovascular and microvascular complications, atherosclerosis, ischemia, hyperemia, shock and hypertension (Gutterman et al., 2005; Webb, 2003). Blood vessels are made of ECs and smooth muscle cells (SMCs) which maintain the

vascular structure and function. The ECs form the blood vessel lumen as they are positioned between the circulating blood and the vessel wall. The SMCs are wrapped around the ECs and generate the force required to constrict or dilate the blood vessels. Acting on either the vascular endothelium, smooth muscle or both, the regulation of vascular tone is achieved by a complicated signaling network involving circulating hormones, neurotransmitters and metabolites (Liu and Gutterman, 2009).

1.10 Effect of MGO on the vasculature

Increased levels of MGO have been observed in patients with vascular diseases. Most of the vascular diseases are associated with initial changes in the vascular permeability followed by structural remodeling of the vasculature. Patients with Type-I diabetes mellitus have a 5-6 fold increase in plasma levels of MGO whereas patients with Type-II diabetes mellitus, have a 2-3 fold increase (McLellan et al., 1994). Previous studies have shown that plasma MGO levels range from 14.2 µM to 33.6 µM in healthy rats (Wang et al., 2004). Several orders of elevation in the MGO levels are expected to take place with persistent hyperglycemia (Chang and Wu, 2006). The MGO levels may be even higher in local tissues than in the plasma as a result of immediate release from cells. Indeed, the MGO levels are as high as 300 µM when measured in cultured mammalian cells (Chaplen et al., 1998). The exact mechanism by which MGO alters the structure and function of the vasculature is unknown. Impaired endothelial dependent vasorelaxation and an increase in the contractility of the vasculature have been observed in human and animal models for hypertension. Dysfunction of the vascular tone is also associated with diabetes, which is characterized by altered metabolic states like hyperglycemia, excess fatty acid availability and insulin resistance. Hyperglycemia causes a decrease in the endothelial nitric oxide (NO) production, and also increases the chances of VSMC proliferation. Being highly

reactive, MGO can react with the –SH and NH_4^+ groups on the proteins present on the VSMCs and ECs on the walls of the blood vessels, thereby interfering with the normal functioning of the vasculature. Altered Ca^{+2} homeostasis has been observed in VSMCs and ECs in animal models treated with MGO (Vasdev et al., 1998). Despite the accumulating evidence for the adverse effects of MGO, the mechanisms and the molecular targets through which MGO regulates the function of VSMs remain to be demonstrated.

1.11 Control of vascular tone

VSMCs are excitable in nature. Membrane potentials of VSMCs determine the muscle contractility (Wray et al., 2005). K_{ATP} channels are present on the plasma membranes of SMCs. Closure of K_{ATP} channels in response to changes in metabolic state causes membrane depolarization. Membrane depolarization leads to the activation of voltage-dependent Ca^{+2} channels (VDCC) raising cytosolic Ca^{+2} levels. The increase in intracellular Ca^{+2} induces the release of more Ca^{+2}. Intracellular Ca^{+2} binds to calmodulin to form a Ca^{+2} – calmodulin complex. This complex binds to myosin light-chain kinase (MLCK) and activates it. Activated MLCK, in turn phosphorylates the myosin light-chain (Herring et al., 2006), which interacts with the actin and causes smooth muscle contraction (Wray et al., 2005). On the contrary, hyperpolarization reduces the activity of the VDCC, lowers the intracellular Ca^{+2} levels, and eventually results in the relaxation of vascular SMCs. Owing to its critical role in maintaining vascular tone, K_{ATP} channel is modulated by a number of vasoactive substances and metabolites.

1.12 K_{ATP} channels

ATP sensitive K^+ channels (K_{ATP}) channels are present on excitable cells like cardiac myocytes, pancreatic β cells, skeletal muscle, vascular SMCs and neurons. Functional K_{ATP} channels are octamers made up of two different types of subunits, four Kir6.x (inwardly

rectifying potassium channel) and four sulphonyl urea receptor (SURx) subunits that belong to the ABC family of transporters. The K_{ATP} channel pore is formed by the Kir6.x (Kir6.1 or Kir6.2) subunits. The Kir6.x subunits consist of two transmembrane domains (TMDs) linked by a pore loop. The SURx subunit exists in two isoforms SUR1 and SUR2. Each SUR isoform has different splice variants. The SURx subunit consists of three membrane spanning domains (MSD) and two nucleotide binding domains (NBDs). ATP binds to the two NBDs in the SUR subunit and is hydrolyzed. ATP hydrolysis by NBD generates the energy required for the conformational change of the MSD domains, which further produce the force required for the gating of the pore forming Kir subunit. K_{ATP} channels are inhibited by ATP and activated by nucleotide diphosphate (NDP) e.g., MgADP. By sensing the ATP and NDP levels, K_{ATP} channels couple cellular metabolism to membrane excitability. Different possible combinations of the Kir6.x and SURx subunits exist, giving rise to a variety of K_{ATP} channels with different physiological roles. Kir6.2/SUR2A channels are observed in cardiac and skeletal muscle whereas Kir6.1/SUR2B channels are found in VSMCs. Disruption of the K_{ATP} channels can have severe consequences as knockout of the Kir6.1 gene in mice leads to coronary vasospasm and sudden death (Chutkow et al., 2002; Miki et al., 2002). In diabetic patients, the vascular response to K_{ATP} channel openers is impaired, resulting in a defect in vasodilation (Desai et al., 2010; Miura et al., 2003).

1.13 Cell's response to stress conditions

A cell responds to stress by regulating several key components of the cellular machinery. Cells respond to stimuli like extreme temperatures, oxidants, inflammation, and exposure to endotoxins, harmful metabolites and genotoxins by implementing a series of adaptive responses known as the cellular stress responses. The main player in the cellular stress response is the

regulation of expression levels of a number of genes. The gene expression can be regulated at the transcriptional level or by post-transcriptional regulatory mechanisms affecting the stability of and translational efficiency of the mRNA (Brennan and Steitz, 2001; Fan et al., 2002). Although cells have mechanisms for the regulation of the mRNA turnover rate to meet their functional needs, transcriptional inhibition and mRNA instability can have severe consequences on cellular function and survival.

1.14 MGO causes a decrease in the expression of vascular K_{ATP} channels

The detrimental effect of MGO has been observed in a range of pathologies. Previously studies were carried out to investigate the role of MGO in the development of vascular complications. Experiments were carried out to test the effect of endogenously produced metabolite MGO on the expression levels of vascular K_{ATP} channels. qPCR experiments were carried out to study the levels of Kir6.1 and SUR2B mRNA in MGO treated A-10 smooth muscle cell line (which endogenously express Kir6.1/SUR2B vascular isoform of the K_{ATP} channels) (Shi et al., 2010). A-10 cells were treated with varying concentrations of MGO for a 12 h period. Following MGO treatment the total RNA was extracted and was subsequently analyzed by regular PCR and qPCR techniques.

Regular PCR analysis showed a clear decrease in the levels of Kir6.1 and SUR2B mRNAs following a 300 µM MGO treatment. Higher doses of MGO (1 mM) lead to nearly a total loss in the levels of Kir6.1 and SUR2B mRNAs. However, the mRNA levels of the internal control GAPDH did not show a significant change in response to similar MGO treatments (Fig. 1A). This suggests that the effect of MGO on the mRNAs is not global but is specific only to Kir6.1 and SUR2B mRNAs. qPCR analysis following MGO treatment showed that the levels of Kir6.1 and SUR2B mRNAs decreased in a concentration dependent manner. The IC_{50} for Kir6.1

and SUR2B mRNAs was found to be 350 μM and 290 μM respectively (Fig. 1B and C). The effect mediated by MGO on the levels of Kir6.1 and SUR2B mRNAs was also found to be time-dependent. The levels of Kir6.1 and SUR2B mRNAs followed a time dependent decrease in response to a 500 μM MGO treatment. The time constant for the mRNA reduction was 1.15 h for Kir6.1 and 0.33 h for SUR2B mRNAs respectively (Fig. 1D and E). (Yang et al., 2011 in review)

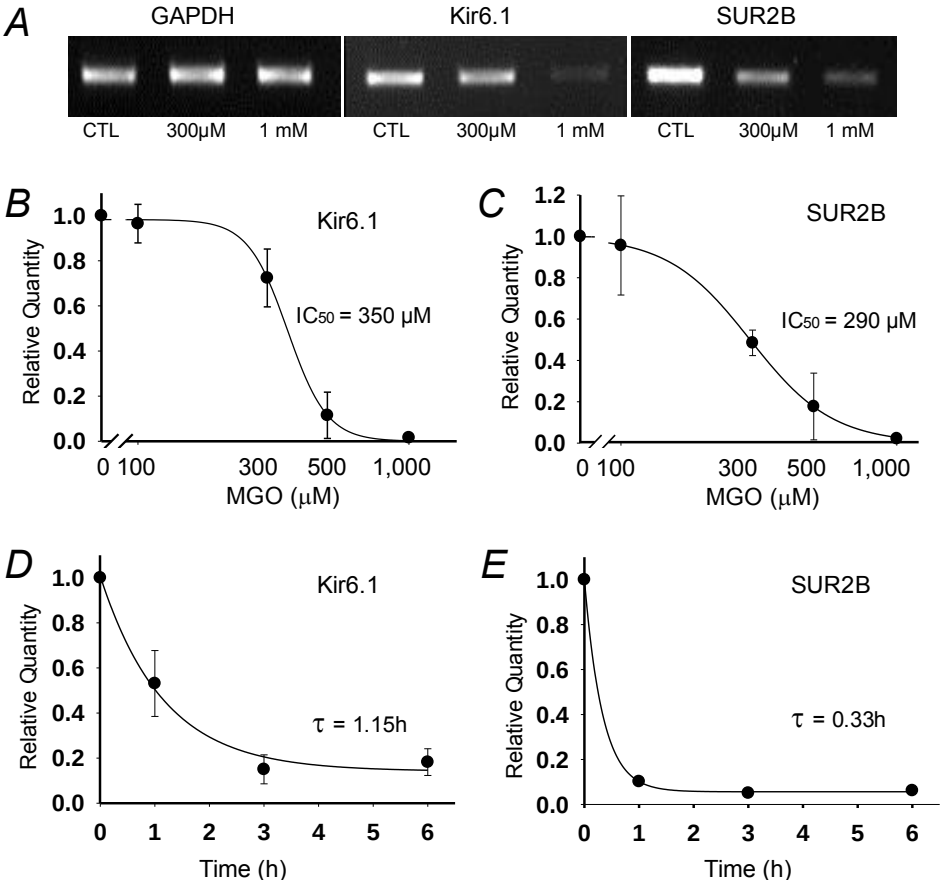

Yang Y, Konduru AS, Trower TC, Shi W, Cui N, Jiang C; J.Biol Chem. (in review)

Figure 1. Prolonged exposure to MGO causes a decrease in the levels of Kir6.1 and SUR2B mRNAs
A. Regular PCR analysis showed a decrease in the levels of Kir6.1 and SUR2B mRNAs on exposure to 300 μM and 1 mM MGO treatment. The levels of GAPDH mRNA showed no detectable change. CTL, control. **B-E.** qPCR analysis of Kir6.1 and SUR2B mRNA following MGO treatment. **B, C.** Reduction in the levels of Kir6.1 and SUR2B mRNA after a 12 h treatment with 300 μM and 1 mM MGO. Kir6.1 IC_{50} = 350 μM and SUR2B IC_{50} = 290 μM. **D, E.** MGO mediated decrease in the levels of Kir6.1 and SUR2B mRNAs followed a time-dependence with a time constant τ, 1.15 h for Kir6.1 and 0.33 h for SUR2B.

1.15 MGO causes a suppression of the vascular K_{ATP} channel currents

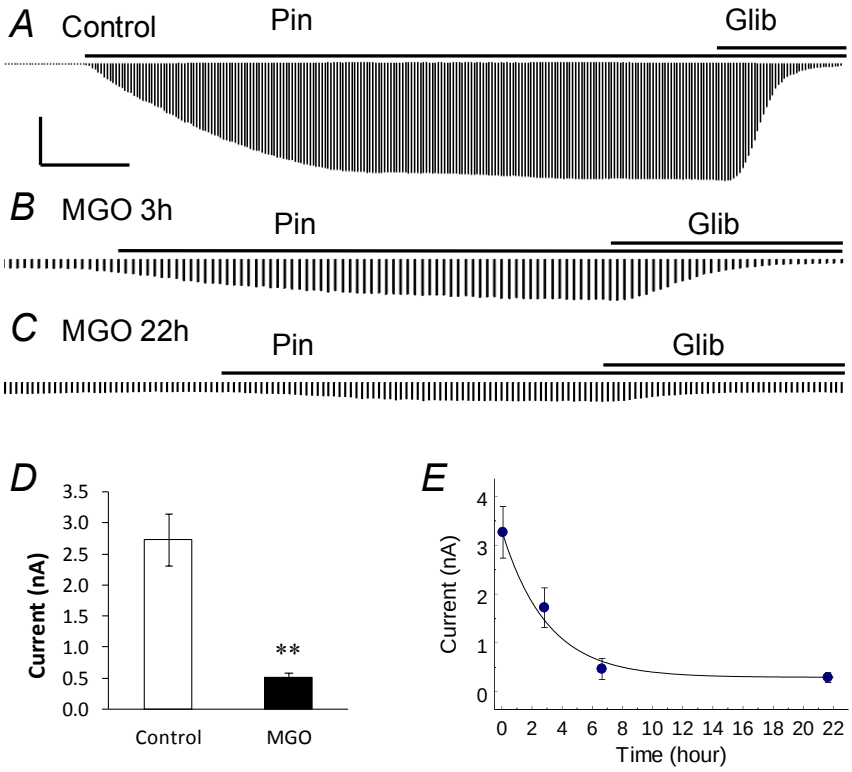

Yang Y, Konduru AS, Trower TC, Shi W, Cui N, Jiang C; J.Biol Chem. (in review)

Figure 2. Prolonged treatments with MGO led to vascular K_{ATP} channel inhibition
A. K_{ATP} channel current activated by pinacidil. **B, C.** Reduction in the pinacidil-induced K_{ATP} channel current in response to 1 mM MGO exposure for 3 h and 22 h respectively. **D.** Summary of the quantitation of pinacidil-induced vascular K_{ATP} channel currents in control and MGO treatment (22 h, 1 mM). **E.** Summary of the quantitation of K_{ATP} channel currents described as a function of time, with the time constant 3 h.

A reduction in the levels of Kir6.1 and SUR2B mRNAs has a major impact on the overall function of the vascular K_{ATP} channels. This was determined by the study of whole cell currents in HEK293 cells in which the vascular Kir6.1/SUR2B channel was heterologously expressed. The K_{ATP} channel currents were activated by an exposure to pinacidil (Pin, K_{ATP} channel opener) (Fig. 2A) that were suppressed by glibenclamide (Glib, K_{ATP} channel blocker), followed by an exposure to 1 mM MGO for 3 h (Fig. 2B). Increasing the MGO exposure time to 22 h nearly abolished the K_{ATP} channel currents (Fig. 2C). Quantitation of the K_{ATP} channel currents after a 1

mM MGO treatment for 22 h showed a ~90% reduction with a 3 h time constant (Fig. 2D and E) which suggests a functional significance of the effect of MGO on the K_{ATP} channel activity (Yang et al., 2011 in review).

1.16 Inhibition of transcription vs. mRNA destabilization

To determine if the decrease in the levels of Kir6.1 and SUR2B mRNAs was due to transcriptional inhibition or mRNA instability further experiments were carried out. A-10 smooth muscle cells with actinomycin D (AcD), a transcriptional inhibitor for different time periods. Subsequent PCR analysis showed that the AcD treatment alone did not cause a decrease in the levels of Kir6.1 and SUR2B mRNAs. When MGO (300 μM) and AcD (5 μg/ml) were applied together, a decrease in the mRNA levels of both Kir6.1 and SUR2B (but not GAPDH) was observed. This effect was similar to the effect shown by MGO treatment alone on Kir6.1 and SUR2B mRNAs. This suggests that MGO mediated decrease in the levels of Kir6.1 and SUR2B mRNAs is not due to suppression of transcription but due to the direct targeting of the K_{ATP} channel mRNAs by MGO (Fig. 3A). (Yang et al., 2011 in review).

Quantitation of the mRNA levels of Kir6.1 showed a decrease in the levels of Kir6.1 mRNA in response to AcD alone whereas a greater extent of reduction was observed following MGO alone treatment (Fig. 3B). The levels of SUR2B mRNA marginally decreased with AcD alone whereas a MGO alone treatment caused a dramatic decrease in the levels of SUR2B mRNA (Fig.3D). However the combined treatment of AcD and MGO did not enhance the reduction kinetics of Kir6.1 and SUR2B mRNAs compared with MGO treatment alone (Fig. 3C and E) suggesting that the decrease in the levels of Kir6.1 mRNA is due to mRNA instability

mediated by the action of MGO but not as a consequence of transcriptional inhibition. (Yang et al., 2011 in review).

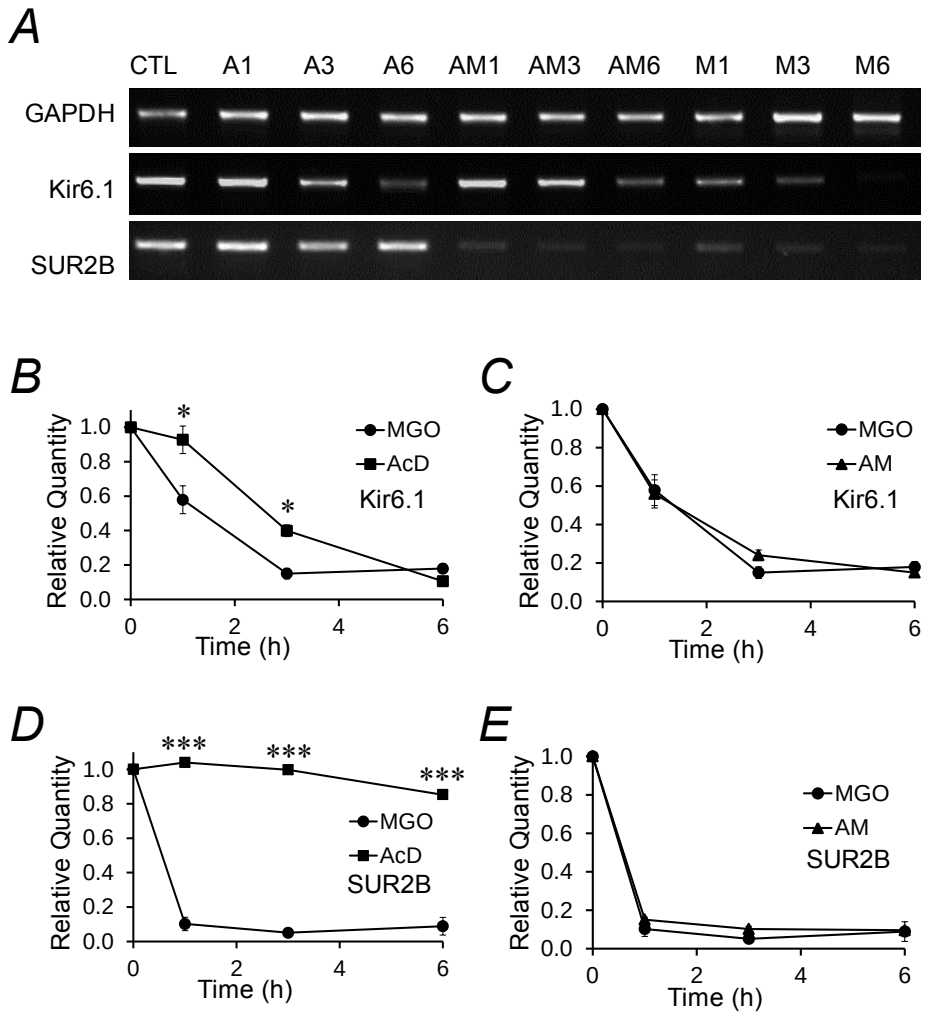

Yang Y, Konduru AS, Trower TC, Shi W, Cui N, Jiang C; J.Biol Chem. (in review)

Figure 3. Inhibition of transcription vs. mRNA destabilization

Inhibition of transcription vs. mRNA destabilization causing a reduction in the levels of Kir6.1 and SUR2B mRNAs. A, Gel images of the reverse transcribed PCR products of GAPDH, Kir6.1 and SUR2B mRNAs from A10 cells treated with AcD (A), AcD and MGO (AM) and MGO alone (M) for different time periods (1, 3 and 6 h, respectively) denoted as a numerical following each treatment condition. CTL, control. *B-E.* qPCR analysis of Kir6.1 and SUR2B mRNAs following AcD, MGO and combined treatment of AcD and MGO (AM) at different time points.

1.17 mRNA stability

The stability of mRNA has a great impact on the response of the cell to a particular stimulus. The mRNA turnover rate can influence the overall protein levels in the cell. The stability of the mRNA is dependent on *cis*-stability elements present on the mRNA and also other *trans*-acting factors. These stability determinants can determine the stability of the mRNA by acting in unison with each other or by acting independently of the other. The *cis*-stability determinants identified on the mRNA are the 5' – guanosine cap, 5' untranslated region (UTR), open reading frame destabilizing sequences, 3'UTR and a stretch of adenosine residues - poly (A) tail.

The 5'guanosine cap present at the 5'end provides resistance to the mRNA from general ribonucleases. This resistance is due to the presence of 5'–5' phosphodiester bond. The removal of the 5'guanosine cap, will make the mRNA vulnerable to the 5'–3' exoribonucleases or endoribonucleases. The 5' UTR sequence also determines the translational efficiency of the mRNA. If the mRNA is bound by ribosomes, and is being translated, the stability of the mRNA increases. In other words, actively translated mRNA is more stable compared to the ones that are not being translated. In addition the 5' UTR can have one or more internal loops that prevent the advancing ribosome to move beyond the loop. The coding region of the mRNA has been identified to have stability determining sequences. *c-fos* mRNA has been identified to have destabilizing sequences in the open reading frame (Shyu et al., 1991). These destabilizing sequences are purine rich sequences and have been identified as targets for at least two cellular proteins. The binding of the cellular proteins to the purine rich sequence initiates mRNA degradation (Chen et al., 1992).

The 3'UTR of the mRNAs has been long studied for their role in determining the stability of the mRNAs. The sequences in the 3'UTR's of the mRNAs can form stem loops that prevent them from being regulated normally. For example the histone mRNA has a 6 bp stem at the near end of the 3' terminal followed a stretch of poly (A). This stem loop was identified to be essential in rendering the histone mRNA stable. It is also possible that some binding proteins might be binding the histone mRNA at the stem loop and thereby causing the stability of the mRNA (Ross, 1995). Conserved stability determining sequences have been identified in the 3' UTRs of different mRNAs. The well-studied stability sequences in the 3'UTRs are the iron responsive element (IRE) present on the iron transporting transferrin mRNA and the stretch of adenylate and uridylate residus (AURE), AUUUA pentamer present in multiple repeats on the mRNAs of cytokines, growth factors and lymphokines. Owing to their presence on the mRNAs coding for important proteins in the cellular function, AUREs are considered important in determining the stability of the mRNAs. The 3'UTR of the *c-fos* mRNA was identified to have an AURE. When the 3'UTR of the *c-fos* mRNA was replaced with the 3'UTR of *v-fos* mRNA, there was an accumulation of the *c-fos* mRNAs following serum stimulation, whereas the *c-fos* mRNA levels dropped significantly when the 3'UTR of *c-fos* was placed downstream of the coding region of *c-fos* indicating that the AURE containing 3'UTR of *c-fos* mRNA was responsible for determining the stability of *c-fos* mRNA. Additionally the AURE can also function as stabilizing signals in many mRNAs. Many cytoplasmic and nuclear proteins have been identified to bind to the AUREs of the mRNAs to influence the stability of the mRNAs (Brennan and Steitz, 2001).

The poly (A) tail of the mRNA has been widely known for conferring stability to the mRNA. Poly (A) tails present at the end of the mRNA was initially thought to give protection to

the 3' terminus of the mRNA from ribonucleases. Deadenylation is the first step in initiating mRNA degradation from the 3'terminus. Poly (A) tails are specifically bound by Poly (A) binding proteins (PABP) that protect the mRNA from deadenylation. In the absence of the poly (A) tail the half lived of mRNAs have been observed to be significantly reduced. It has also been determined that poly (A) tails increases the translational efficiency of the mRNA by interacting with the translation initiation and elongation factors docked at the 5' terminus of the mRNA. The stability of the mRNA increases, when the mRNA is actively transcribed. Thus in the absence of poly (A) tail the translational efficiency would be compromised leading to a decrease in the stability of the mRNA (Ross, 1995).

In addition to the *cis*-stability determinants present on the mRNA, several *trans*-acting factors like ions, growth factors, hormones, metabolites can also affect the stability of the mRNA by binding to the *cis*-stability determinants (Sachs, 1993).

1.18 Significance

Although MGO is known to be a major player in vascular complications and vascular inflammation state, its vascular targets and mechanisms of action are still unclear. The membrane proteins responsible for maintaining the contractility, membrane potentials and membrane properties of the ECs and VSMCs can be regulated by MGO. The vascular K_{ATP} channel is a potentially important target of MGO in vasculatures. Disruption of functional K_{ATP} channels will lead to abnormalities in cellular excitability, VSM contraction and impairment of vascular responses to vasoconstrictors and vasodilators. Therefore, we performed these studies to test the hypothesis that MGO affects the function of vascular K_{ATP} channels by destabilization of Kir6.1 and SUR2B mRNAs because MGO is known to preferentially bind to and react with single stranded nucleotides. Our results showed that MGO treatment caused disruption of both

Kir6.1 and SUR2B mRNAs through two distinct mechanisms. Such an effect is likely to impair membrane potentials and K^+ homeostasis of VSMs thereby causing vascular dysfunction, seen in many vascular diseases. Membrane potential appears to be one of the mechanisms (Liu and Gutterman, 2002) that can lead to a disruption of the cellular homeostasis. Depolarization can open the voltage-activated Ca^{2+} channels leading to Ca^{2+} influx (Anzai et al., 2000; Wray et al., 2005). Since K^+ channels are the primary regulators of membrane potentials, inhibition of the K^+ channels results in depolarization and an elevation in intracellular Ca^{2+} (Cook et al., 1988). Since several NADPH oxidases for ROS production are stimulated by elevated intracellular Ca^{2+} (Brandes et al., 2010; Guzik et al., 2008; Hink et al., 2001; Zhang et al., 2008), and since RCS and ROS share the antioxidant detoxification systems, sustained depolarization may augment the production of these reactive species and aggravate oxidative/carbonyl stress. Thus the understanding of the regulation of vascular tone will have a strong influence on designing treatments for the vascular diseases.

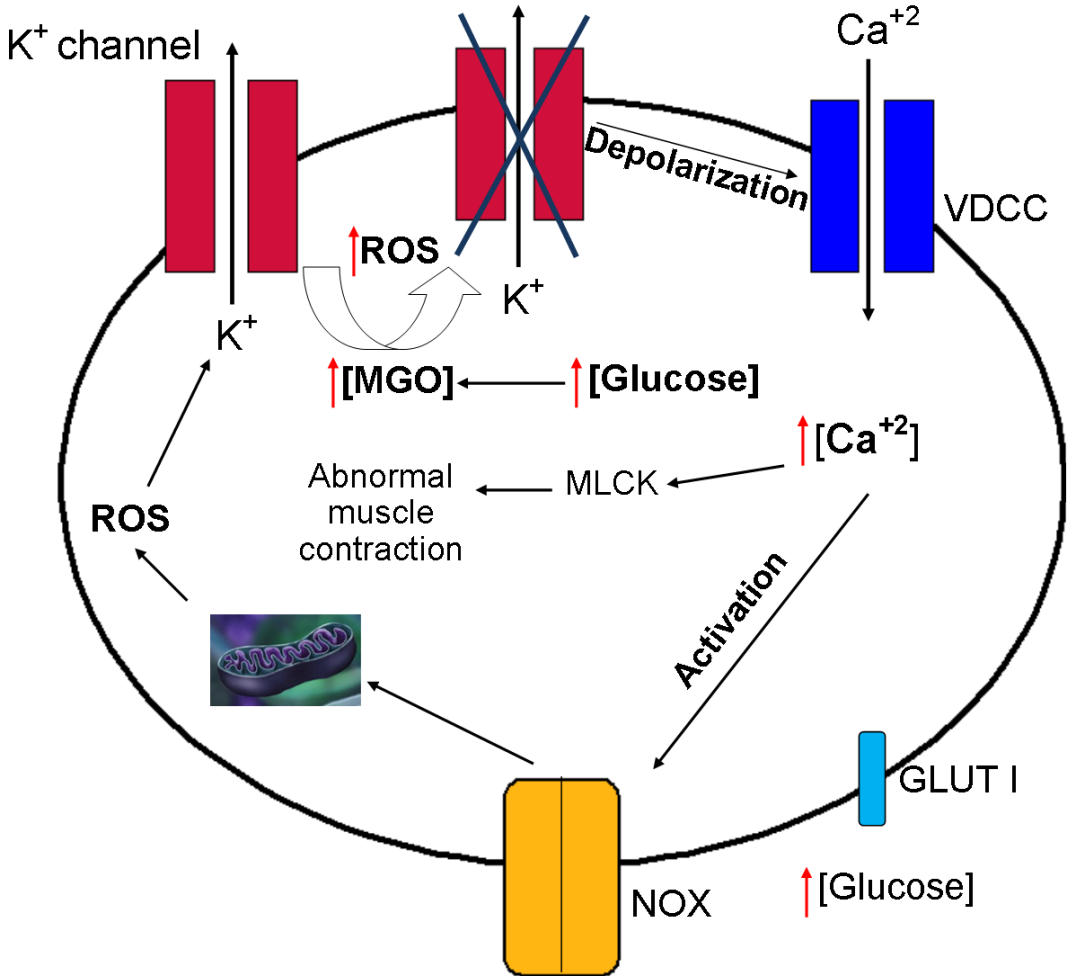

Figure 4. Working hypothesis summarizing the effect of MGO on cellular homeostasis

Hyperglycemia leads to the production of MGO. MGO causes a reduction in the expression levels of vascular K_{ATP} channels by causing mRNA instability of Kir6.1 and SUR2B mRNAs. Loss of functional K_{ATP} channels causes depolarization of the membrane potential, which in turn activates voltage dependent calcium channels (VDCC). Activated VDCC leads to an influx of Ca^{+2} into the cytosol. Increased cytosolic Ca^{+2} activates the Ca^{+2} dependent NADPH oxidase (NOX), which aids in the production of ROS from the mitochondria. ROS produced can further modulate the K_{ATP} channels and thereby augment the existing carbonyl and oxidative stress. Increased cytosolic Ca^{+2} can also lead to abnormal SMC contractility. Glucose is transported into the cell by the GLUT I, glucose transporter.

2. MATERIALS AND METHODS

2.1 Genomic DNA isolation

Sprague Dawley rat (Jackson lab) tail tissue was used for isolating the genomic DNA using the DNeasy Blood and Tissue kit (Qiagen) following manufacturer's protocol.

2.2 Amplification of the 3' UTR's of Kir6.1 and SUR2 mRNA

Primer pairs with a 5'–XhoI overhang for the 3' UTRs of Kir6.1/SUR2 genes were designed based on the conserved sequences from rat genomic sequence (Accession no.AC_000072.1). PCR was performed in a 20 µl reaction containing 1 µg of isolated genomic DNA, 0.75 mM dNTPs, 2.5 µl DMSO, Pfu ultra buffer at final concentration of 1X, 25 nM of primer mixture, 1 µl of Pfu ultra DNA polymerase using Mastercycler (Eppendorf Pro S) with an initial denaturation period of 95 °C for 2 min, followed by 36 cycles of denaturation at 95 °C for 50 s, annealing at 60 °C for 45 sec, and extension at 72 °C for 2 min, with a final elongation at 72 °C for 10 min. The PCR products were analyzed on a 2% agarose gel.

Table 1: List of primers for amplification of the 3'UTRs of Kir6.1 and SUR2B mRNAs

Target gene	Accession No.	Primer sequence	Amplicon length (bp)
Kir6.1	NM_017099.3	Fw: ACCGCTCGAGCCTCCATCCGGAGGAATAAC Re: ACCGCTCGAGCGTCTTCACAAGACTCCCACAC	1000
SUR2	NM_013040.2	Fw: ACCGCTCGAGCGCTGACCTGGTCATTGTGATG Re: ACCGCTCGAGCGCAGGTGAATCCTACCGATAC	2600

Note: Primers were designed to include the ACCGCTCGAG overhang. Xho I consensus sequence is underlined.

2.3 pmirGLO luciferase reporter vector

The pmirGLO expression vector (Promega) was designed to quantitatively evaluate the effect endogenously present or exogenously introduced compounds/factors on a specific gene. The vector backbone includes a firefly luciferase gene (luc2) under the control of PGK promoter, a multiple cloning site (MCS) downstream of luc2. Additionally the vector contains a renilla (hRluc-neo) gene under the control of SV40 promoter. The gene of interest to be studied for targeting by miRNAs or other compounds is cloned downstream of luc2 gene. luc2 serves as a primary reporter gene, a decrease in the firefly luciferase expression indicates that the gene cloned into the reporter vector is targeted by compound/factor under study. hRluc-neo gene serves as a control reporter for normalization process.

2.4 Cloning of the 3'UTRs of Kir6.1 and SUR2B mRNA to pmirGLO luciferase reporter vector

The pmirGLO expression was digested with XhoI restriction enzyme (restriction site located downstream of the firefly - luc2 gene) and gel purified with QIAquick gel extraction kit (Qiagen) according to the manufacturer's instructions. The appropriate PCR products for 3'UTR of Kir6.1 and SUR2B were purified using the QIAquick PCR purification kit (Qiagen). The purified fragments were digested with XhoI enzyme followed by purification of the digested fragments. Ligation was performed in a 10 µl volume, 50 ng of digested vector and 300 ng of digested fragment were incubated with 400 U of T4 DNA ligase (M0202S, NEB) for 16 h at 16 °C. The ligated products were transformed into XL1-blue competent cells (Agilent) for amplification and the amplified DNA was obtained through plasmid Mini-preparation (Qiagen). The constructs were confirmed by DNA sequence analysis.

2.5 Cell culture

Rat vascular smooth muscle cells (A-10, CRL-1476, ATCC, Manassas, VA) were cultured as a monolayer and grown to 80-90% confluence in a 35 mm petri dish in DMEM/10%FBS in a humidified 5% CO_2 atmosphere at 37 °C.

2.6 Transfection of A-10 cells and MGO treatment

A 35 mm petri dish of cells was transfected with 1 µg Kir6.1 or SUR2B 3'UTR containing pmirGLO luciferase reporter vector using Fugene 6 transfection reagent (Roche Applied Science, Indianapolis, IN). The cells were dissociated with trypsin (0.25%) after 8-12 h of transfection and were seeded into 96-well plate for further growth. MGO treatment (in triplicates) was performed after 18-24h. The cells were treated with 75 µl of 10, 30, 100 and 300 µM MGO freshly prepared in DMEM/10%FBS for 5 h following which luciferase reporter assay was performed.

2.7 Luciferase assay

Luciferase reporter assay was performed using the Dual-Glo luciferase assay system (Promega), 5 h after the MGO treatment. Briefly, a 75 µl of Dual-Glo substrate equal to the volume of the MGO containing culture medium was added to each well and mixed. The firefly luminescence was measured using a luminometer (Model 1420 Victor3V, Perkin Elemer, Waltham, MA) after a 15-20 min incubation period. After obtaining the firefly luciferase reading, 75 µl of Dual Glo Stop & Glo reagent equal to the volume of original culture medium was added to each well and the renilla luminescence was measured after 15-20 min. The ratio of firefly: renilla luciferase was calculated for each well. The sample well ratio was normalized to the control well ratio.

2.8 *In vitro* transcription of Kir6.1 and SUR2B genes

cDNA sequences of rat Kir6.1 (GenBank™ No. D42145) and mouse SUR2B (GenBank™ No. D86038, mRNA isoform NM_011511) were previously cloned into pcDNA 3.1cloning vector. Linear template DNA required for *in vitro* transcription experiments was obtained by using a restriction site downstream of the cDNA insert on the pcDNA 3.1. The *in vitro* transcription reactions were performed in RNase free environment with MEGAscript T7 high yield transcription kit (Ambion). For the *in vitro* transcription reaction, 1 µg of linearized template DNA was incubated with 8 µl of the NTP mixture, 2 µl of 10X reaction buffer and 2 µl of T7 enzyme mix in a 20 µl reaction at 37 °C for 4 h. The *in vitro* transcribed RNA was recovered by adding 30 µl of Lithium chloride precipitation solution to the *in vitro* transcription reaction mixture and chilled at -20 °C for 4 h. The RNA was pelleted by centrifugation at 4 °C for 15 min at 13,000 rpm. The RNA pellet was washed once with 70% ethanol, re-centrifuged and the supernatant was discarded. The RNA pellet was dissolved in appropriate volume of RNase free H_2O.

2.9 Exposure of *in vitro* transcribed Kir6.1 or SUR2B mRNA to MGO

MGO was diluted to the required concentrations in RNase free H_2O from a 5.5 M stock solution. For the MGO treatment, 2 µg of RNA was treated with 10 µl of MGO (100, 300 and 600 µM) at 37 °C for 6, 18 or 24 h time periods.

2.10 Determination of the effect of MGO on Kir6.1 or SUR2B mRNA

After MGO treatment, 95% formamide containing gel loading buffer was added to the MGO + RNA mixture and heat denatured at 65 °C for 45 min followed by chilling on ice. The denatured RNA was resolved on a 1.5% agarose gel and visualized with ethidium bromide under

UV-fluorescence. The RNA band intensity on the gel was determined by densitometry analysis using ImageJ (Abramoff, 2004).

2.11 Data Analysis

Data are presented as the mean ± S.E. Differences in means tested with Student's *t* test or analysis of variance (ANOVA) and were accepted as significant if $P \leq 0.05$.

3. SPECIFIC AIM

To demonstrate that MGO exposure causes a disruption of the mRNAs of Kir6.1 and SUR2B subunits of the vascular isoform of the K_{ATP} channels, leading to impairment of function K+ currents.

This aim was addressed by a series of studies. The 3' UTR of mRNA is considered to be a major determinant of the stability of the mRNA. The 3' UTRs of Kir6.1 and SUR2B mRNAs were amplified from the respective genomic DNA and cloned to a luciferase reporter vector (pmirGLO) to study the effect of MGO on the 3' UTRs of Kir6.1 and SUR2B mRNAs. In addition to the 3' UTR, the coding region and 5' UTR of the mRNA are also known to contribute to the stability of the mRNA. The mRNAs of Kir6.1 and SUR2B subunits of the vascular K_{ATP} channel were synthesized by *in vitro* transcription reactions. The *in vitro* synthesized mRNAs were treated with varying concentrations of MGO and the effect of MGO on the mRNAs of Kir6.1 and SUR2B was determined by resolving the MGO treated mRNAs with gel electrophoresis and the mRNA bands were visualized under UV-fluorescence. The variation in the mRNA bands of MGO treated and non-treated samples was quantified using ImageJ, an image processing program.

4. RESULTS

4.1 MGO acts on the 3'UTR of K_{ATP} channel mRNAs

The stability of a mRNA largely relies on its 3' UTR (Ross, 1995). To study the effect of MGO on the 3' UTR of Kir6.1 and SUR2B mRNAs, a luciferase reporter vector was used. The 3'UTRs of Kir6.1 and SUR2B were cloned into the pmirGLO luciferase vector and the A-10 cells were transfected with Kir6.1 or SUR2B 3'UTR containing luciferase vector. The effect of MGO on the luciferase expression in the transfected cells was determined with Dual-Glo luciferase assay system, 5 h after MGO (10, 30, 100 and 300 μM) treatment.

A-10 cells transfected with Kir6.1-3'UTR containing luciferase vector, showed a concentration-dependent reduction in the luciferase reporter signal (Fig. 5A). A treatment with 300 μM MGO led to a maximum decrease in the luciferase activity in the A-10 cells by 28.8 ± 5.3% ($P < 0.001$; $n = 5$) compared with the control. The difference in the luciferase activity observed in the cells treated with MGO from that of the control luciferase activity was statistically significant. A decrease in the luciferase activity by 15.2 ± 2.9% ($P < 0.05$; $n = 5$) and 4.5 ± 3.5% ($n = 4$) was observed in A-10 cells treated with 100 μM and 10 μM MGO, respectively.

In contrast, A-10 cells transfected with SUR2B-3'UTR containing luciferase vector did not show a similar response to the same set of MGO treatments. The decrease in the luciferase activity in response to MGO treatment was not statistically significant (Fig. 5B).

Therefore, it is likely that MGO acts on the 3'UTR of Kir6.1 mRNA causing its instability while MGO may mediate its effect on SUR2B mRNA stability via a different mechanism instead.

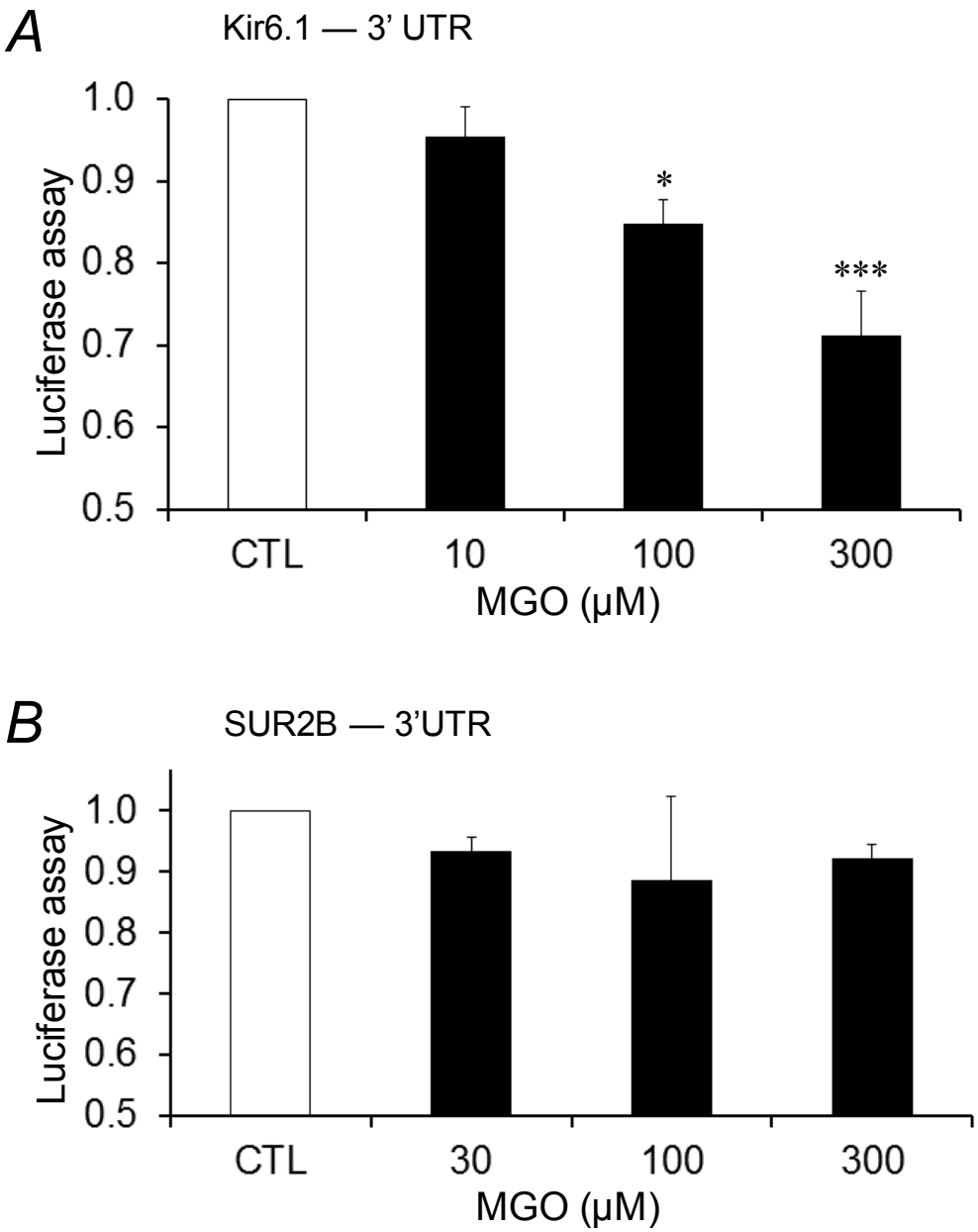

Figure 5. MGO acts on the 3'UTRs of K_{ATP} channel mRNAs

A-10 cells transfected with Kir6.1-3'UTR or SUR2B-3'UTR containing luciferase reporter vector (pmirGLO) were treated with different concentrations of MGO respectively and the luciferase gene expression from the reporter vector was measured after 5 h. The ratio of firefly (experimental reporter) : renilla (control reporter) luciferase was calculated for each well. The sample well ratio was normalized to the control well ratio and is represented on the Y- axis as the amount of luciferase activity in response to different MGO treatments along with the control. **A.** Summary of the effect of different concentrations (10 μM, 100 μM and 300 μM) of MGO on the luciferase activity of Kir6.1-3'UTR containing luciferase reporter vector. **B.** Summary of the effect of different concentrations (30, 100 and 300 μM) of MGO on the luciferase activity of SUR2B-3'UTR containing luciferase reporter vector. *, $P < 0.05$; ***, $P < 0.001$; n = 4 experiments.

4.2 MGO suppresses the activity of K_{ATP} channels by directly acting on regions other than the 3'UTRs on Kir6.1 and SUR2B subunit mRNAs

Since MGO has been shown to interact directly with nucleic acids (Krymkiewicz, 1973) to form adducts, we tested the possibility that the coding sequences of the Kir6.1/SUR2B mRNA are targeted by MGO, leading to mRNA degradation. Kir6.1 and SUR2B mRNAs synthesized by *in vitro* transcription reactions were then treated with 100, 300 and 600 μM MGO for 18 h time period. The change in the mRNA levels of Kir6.1 and SUR2B following MGO treatment was resolved by gel electrophoresis and visualized with ethidium bromide under UV-fluorescence.

Obvious reduction in the band density of SUR2B mRNA was seen with 300 μM MGO treatments, and the decrease in the SUR2B mRNA band was more prominent with 600 μM MGO treatment (Fig. 6B *top panel*). MGO mediated mRNA instability may also result in a reduction in the size of the mRNA. Thus, we elongated the image obtained from UV-fluorescence in a vertical orientation to determine if there is any difference in the migration distance of MGO treated mRNA samples compared with the control. This shows that SUR2B mRNA treated with 600 μM MGO migrated a slightly longer distance compared with that of control mRNA (Fig. 6B *bottom panel*) and hence the mRNA band lay lower on the gel with respect to the control band. This indicates that SUR2B mRNA may be degraded upon MGO treatment and thus resulted in a band slightly smaller in size compared with the control.

Similar experiments were also performed on *in vitro* transcribed Kir6.1 mRNA. Kir6.1 mRNA treated with increasing doses of MGO does not show a significant change in the RNA levels compared with the control (Fig. 6A)

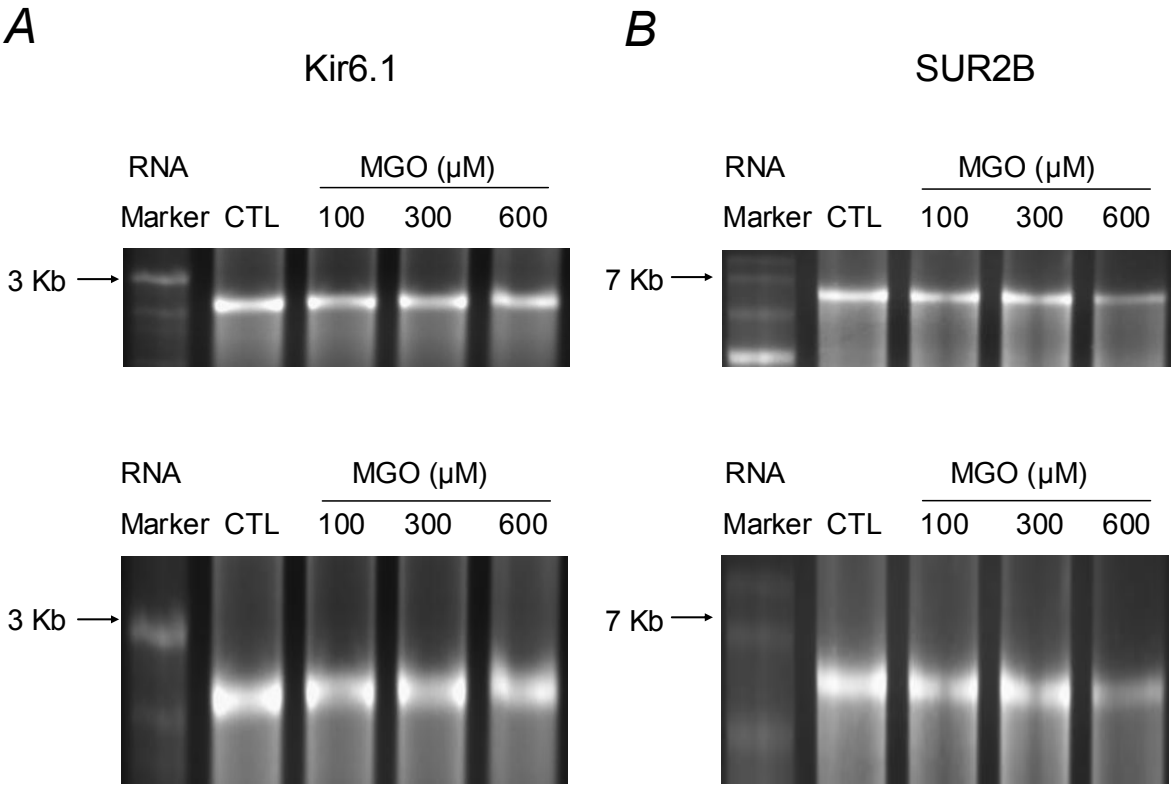

Figure 6. MGO suppresses the activity of K_{ATP} channels by directly acting on regions other than the 3'UTRs on Kir6.1 and SUR2B subunit mRNAs

Kir6.1 and SUR2B mRNAs were synthesized by *in vitro* transcription reaction and were treated with different concentrations of MGO. **A, B.** (*top panel*) Gel image of Kir6.1 and SUR2B mRNAs treated with 100 μM, 300 μM and 600 μM MGO respectively, along with untreated mRNA, control (CTL) for 18 h obtained from UV – fluorescence. (*bottom panel*) Vertical elongation images of Kir6.1 and SUR2B gel images from the corresponding top panels. The dashed line represents the position of the band from the control sample, at which the mRNA bands were analyzed for change in migration distance and density. The RNA band sizes on the RNA marker are labeled.

Taken together these results suggest that MGO acts on the mRNAs of SUR2B subunit at regions other than the 3' UTR and causes a decrease in the SUR2B mRNA levels, whereas a significant decrease in mRNA levels of Kir6.1 subunit was not observed.

4.3 MGO mediates dose dependent decrease in the levels of SUR2B mRNA

The decrease in the mRNA levels of SUR2B following MGO treatment was noted if the density of the mRNA bands from MGO treated samples decreased compared with the control sample following gel electrophoresis and visualization with UV- fluorescence. The change in the mRNA band density in MGO treated mRNA samples compared with the control sample was quantified using by densitometry analysis of the RNA bands using ImageJ image processing program.SUR2B mRNA was treated with increasing concentrations (100, 300 and 600 μM MGO) for different time points.

Following a 6 h MGO exposure a marginal decrease in the levels of SUR2B mRNA band density was observed in response to increasing concentrations of MGO (Fig. 7A). A decrease in the band density by 4.6 ± 0.8% (n = 4) was observed with 100 μM MGO treatment. A further increase in the MGO concentration to 300 and 600 μM, lead to a decrease in the mRNA band density by 6.9 ± 1.0% (n = 4) and 7.7 ± 1.5% (n = 4) respectively.

At an 18 h time point (Fig. 7B), a 600 μM MGO treatment led to a pronounced decrease in the SUR2B mRNA band density compared to the control value (61.4 ± 3.2%, $P < 0.001$; n = 4). Treatment with lower concentrations of MGO produced a smaller, but significant decrease by 43.4 ± 6.4% ($P < 0.001$; n = 4) with 300 μM MGO whereas a 14.4 ± 2.9 % (n = 4) decrease was observed with 100 μM MGO.

At 24 h time point (Fig. 7C), a 600 μM MGO treatment lead to a drastic decrease in the levels of SUR2B mRNA by 84.3 ± 1.2% ($P < 0.001$; n = 4) compared with the control. Treatment with lower concentrations of MGO produced a decrease in the SUR2B mRNA band density by 68.0 ± 4.4% ($P < 0.001$; n = 4) with 300 μM and 50.1 ± 7.1% ($P < 0.001$; n = 4) with 100 μM MGO.

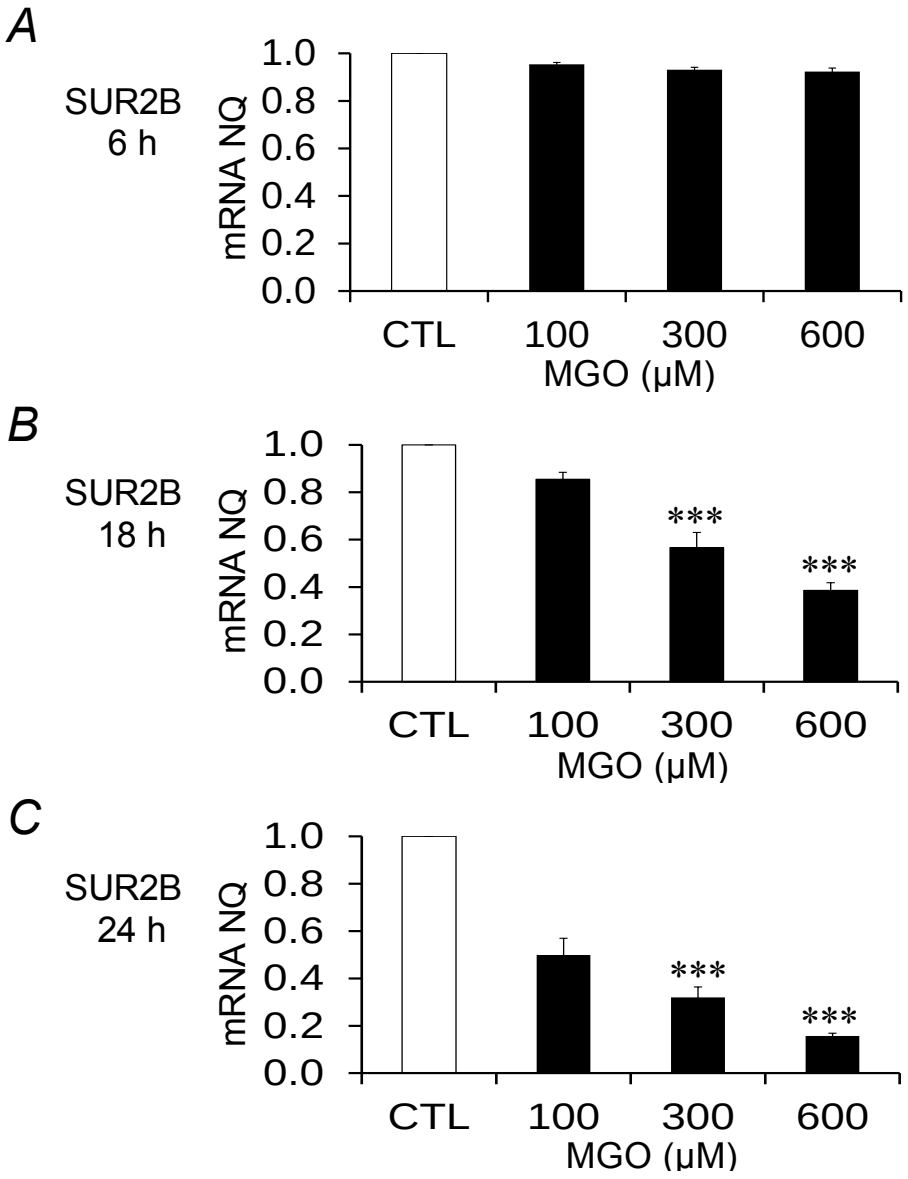

Figure 7. MGO mediates dose dependent decrease in the levels of SUR2B mRNA
Summary of Net quantitation (NQ) of SUR2B mRNA following MGO treatment (100, 300, and 600 μM). **A.** Exposure time 6 h. **B.** Exposure time 18 h. **C.** Exposure time 24 h. ***, $P < 0.001$; n = 4 experiments.

Taken together, these results suggest that MGO mediated decrease in the levels of SUR2B mRNA is dependent on the concentration of MGO. Higher concentration (600 μM) of MGO leads to a greater reduction in the density of the SUR2B mRNA band compared with 300 μM and 100 μM MGO treatment.

4.4 SUR2B mRNA levels decrease with an increase in the MGO exposure time

To determine the time-dependence for the effect of MGO on SUR2B mRNA levels, SUR2B mRNA was treated with 300 and 600 µM MGO for 6, 18 and 24 h (Fig. 8).

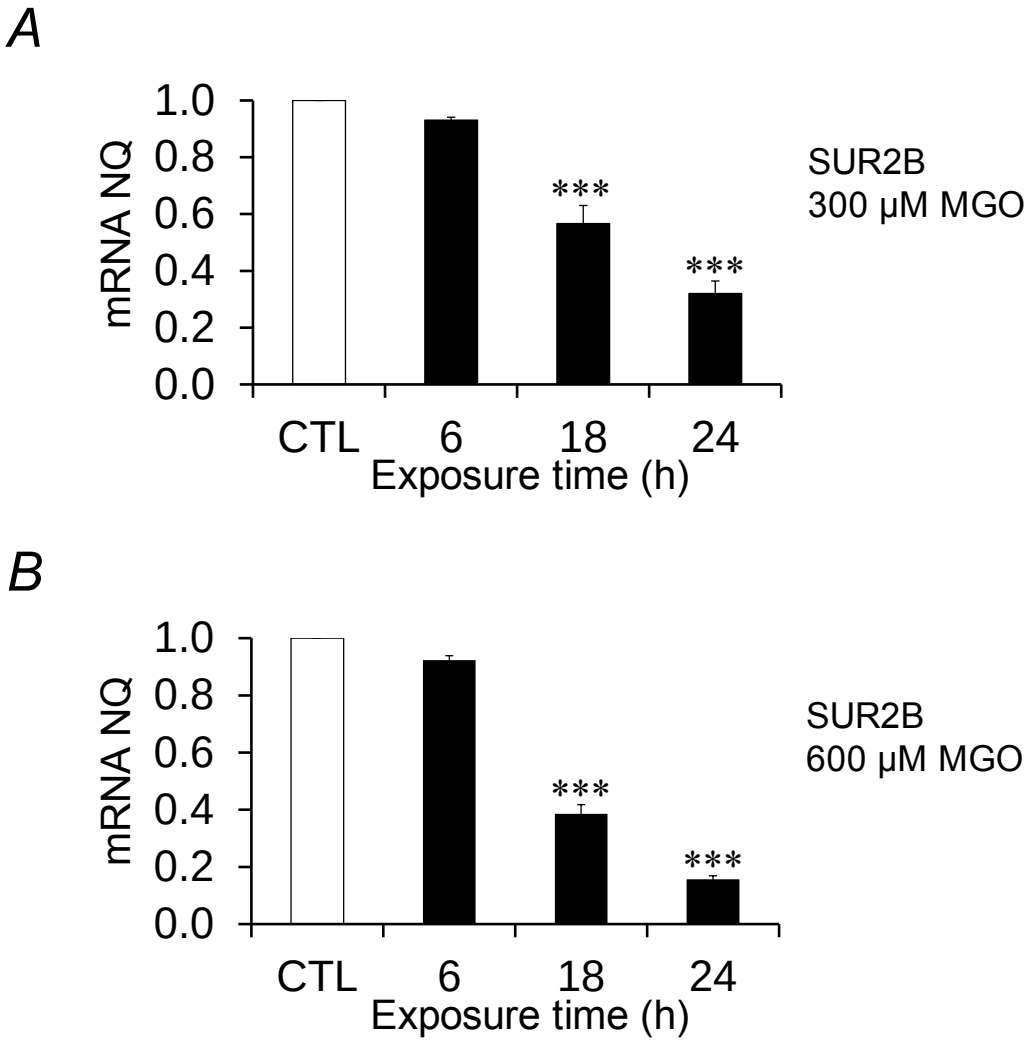

Figure 8. SUR2B mRNA levels decrease with an increase in the MGO exposure time
Summary of NQ of SUR2B mRNA at different exposure times (6, 18 and 24 h) following MGO treatment. **A.** MGO concentration, 300 µM. **B.** MGO concentration, 600 µM. ***, $P < 0.001$; $n = 4$ experiments.

A 300 µM MGO treatment (Fig. 8A) caused a marginal decrease in the levels of SUR2B mRNA by 6.9 ± 1.0% (n = 4) after a 6 h MGO exposure, while an exposure to MGO for 18 h and

24 h caused graded decreases in the SUR2B mRNA levels by 43.4 ± 6.4% ($P < 0.001$; n = 4) and 68.0 ± 4.4% ($P < 0.001$; n = 4), respectively.

With a 600 μM MGO treatment (Fig. 8B), a similar pattern of reduction compared to the 300 μM MGO treatment was observed after 6, 18 and 24 h exposure times. A slight decrease in the levels of SUR2B mRNA by 7.7 ± 1.5% (n = 4) after a 6 h MGO exposure, while the MGO exposure for 18 h and 24 h enhanced the reduction in SUR2B mRNA levels by 61.4 ± 3.2% ($P < 0.001$; n = 4) and 84.3 ± 1.2% ($P < 0.001$; n = 4), respectively.

4.5 Effect of increasing doses of MGO on Kir6.1 mRNA

MGO experiments similar to the ones performed on SUR2B mRNAs were also performed on the Kir6.1 mRNAs. Kir6.1 mRNA was treated with increasing concentrations (100, 300 and 600 μM) of MGO for 6, 18 and 24 h time periods.

Following a 6 h MGO exposure, a marginal decrease in the levels of Kir6.1 mRNA band density was observed in response to increasing concentrations of MGO (Fig. 9A). A decrease in the band density by 2.4 ± 1.3% (n = 3) was observed with 100 μM MGO treatment. A further increase in the MGO concentration did not lead to a further change in the mRNA band density (2.4 ± 1.7%, n = 4 with 300 μM and 2.4 ± 0.7%, n = 4 with 600 μM respectively).

At an 18 h time point (Fig. 9B), a 3.4 ± 1.1 % (n = 4) decrease in the Kir6.1 mRNA band compared with the control value was observed following a 100 μM MGO treatment. An increase in the MGO dose to 300 and 600 μM led to a slight decrease in the density of Kir6.1 mRNA bands by 4.7 ± 1.0% (n = 4) and 5.5 ± 1.3% (n = 4) respectively compared to the control.

At 24 h time point (Fig. 9C), a 100 μM MGO treatment lead to decrease in the levels of Kir6.1 mRNA by 8.5 ± 3.0% (n = 4) compared with the control. Treatment with higher

concentrations of MGO produced a decrease in the Kir6.1 mRNA band density by 11.8 ± 2.4% (n = 4) with 300 μM and 19.1 ± 2.9% (n = 4) with 600 μM MGO treatments.

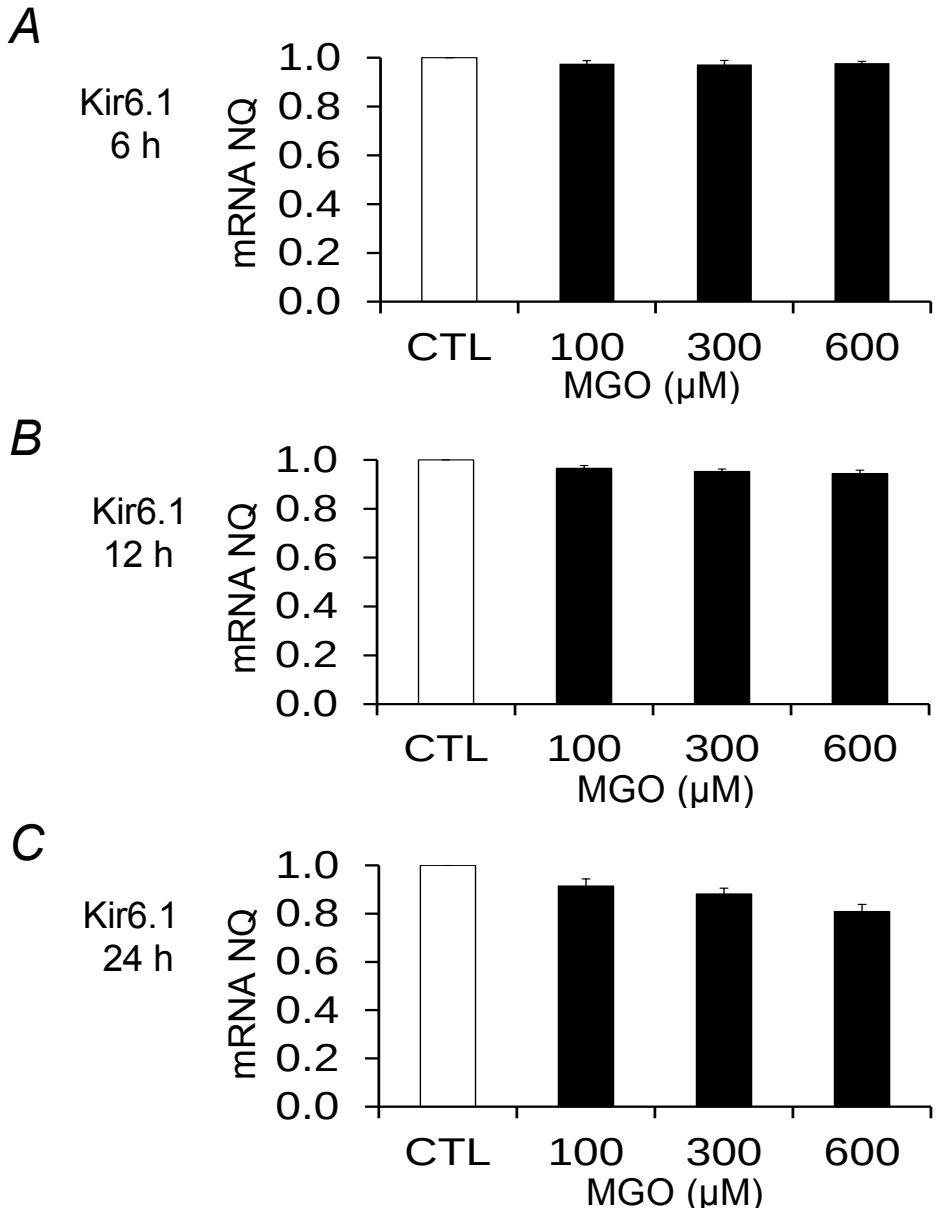

Figure 9. Effect of increasing doses of MGO on Kir6.1 mRNA
Net quantitation (NQ) of Kir6.1 mRNA following MGO treatment (100, 300, and 600 μM). **A.** Exposure time 6 h. **B.** Exposure time 18 h. **C.** Exposure time 24 h. n = 4

The difference in the Kir6.1 mRNA band densities observed between 100, 300 and 600 μM MGO treatments was not significant ($P > 0.05$). These results suggest that MGO does not

have an effect on Kir6.1 mRNAs. Increasing the MGO concentrations do not lead to a significant change in the Kir6.1 mRNA band density.

4.6 Effect of MGO on Kir6.1 mRNA at different exposure times

To determine the time-dependence for the effect of MGO on Kir6.1 mRNA levels, Kir6.1 mRNA was treated with 300 and 600 µM MGO for 6, 18 and 24 h (Fig. 10).

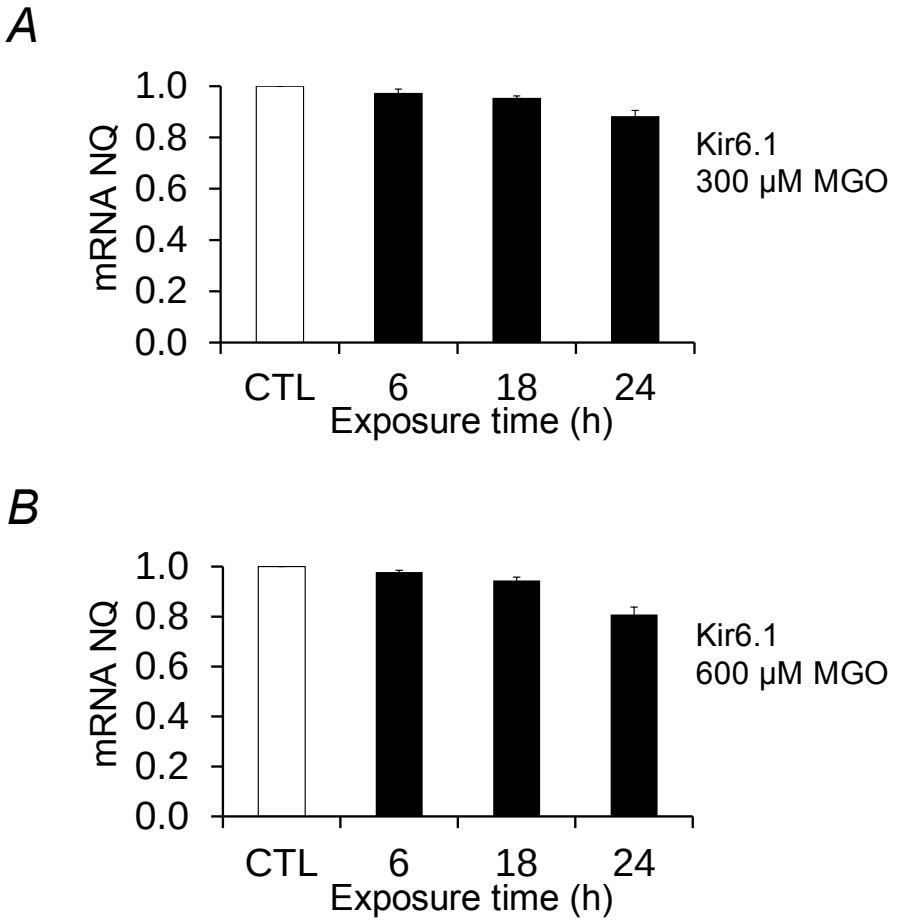

Figure 10. Effect of MGO on Kir6.1 mRNA at different exposure times
Net quantitation (NQ) of Kir6.1 mRNA at different exposure times (6, 18 and 24 h) following MGO treatment. **A.** MGO concentration, 300 µM. **B.** MGO concentration, 600 µM. n = 4.

A 300 µM MGO treatment (Fig. 10A) caused a marginal decrease in the levels of Kir6.1 mRNA by 2.8 ± 1.7% (n = 3) after a 6 h MGO exposure, while the an increase in the MGO

exposure time to 18 h caused a slight decrease in the Kir6.1 mRNA levels by 4.7 ± 1.0% (n = 4) and to 24 h caused a decrease in the mRNA band density by 11.8 ± 2.4% (n = 4).

With a 600 μM MGO treatment (Fig. 10B), a significantly different pattern in the reduction of Kir6.1 mRNA levels compared to 300 μM MGO treatment was not observed, following a 6, 18 and 24 h exposure times. A slight decrease in the levels of SUR2B mRNA by 2.2 ± 0.7% (n = 3) after a 6 h MGO exposure, while the MGO exposure for 18 h and 24 h enhanced the reduction in Kir6.1 mRNA levels by 5.5 ± 1.3% (n = 4) and 19.1 ± 2.9% (n = 4), respectively.

The reduction observed in Kir6.1 mRNA band density was not significant ($P > 0.05$) thereby suggesting that MGO does not act on the Kir6.1 mRNA to cause a reduction in Kir6.1 mRNA levels.

Taken together these results suggest that MGO acts on the vascular K_{ATP} channels by decreasing the expression of K_{ATP} channels. MGO acts on the 3'UTR of Kir6.1 mRNA and the coding region of the SUR2B mRNA to cause a decrease in the levels of K_{ATP} channel mRNAs.

5. DISCUSSION

In the present study, we have found evidence for the disruption of vascular K_{ATP} channels with an MGO exposure, and shown the underlying mechanisms. MGO treatment causes a major reduction in the Kir6.1 and SUR2B mRNAs and impairs activity of the K_{ATP} channels. Remarkably, MGO appears to act on the 3'UTR of the Kir6.1 gene and the coding region of the SUR2B gene, leading to mRNA instability and a loss of functional K_{ATP} channels in plasma membranes.

Emerging evidence suggests that RCS including MGO play a major role in the development of diabetic complications in multiple organs and systems (Bourajjaj et al., 2003). Like ROS, RCS are highly reactive, and can modify proteins, DNAs and lipids via Maillard covalent links, producing advanced glycation end products (AGEs) (Thornalley et al., 1999). AGEs can cause direct damages to intracellular cellular structures and act on extracellular AGE receptors, producing more reactive species in the cytoplasm through intracellular signaling systems (Brownlee, 2001). When the cellular mechanisms for the detoxification of the RCS are overwhelmed by their production, the so-called carbonyl stress takes place. The carbonyl stress has been suggested playing even more important role than oxidative stress in the development of diabetic vascular complications (Ellis, 2007).

Although the production of RCS is normally controlled by antioxidants, scavengers and their degrading enzymes, there are circumstances when key molecules for the maintenance of homeostatic states become defective or dysfunctional, allowing these reactive species to be overly produced. Membrane potential appears to be one of such mechanisms (Liu and Gutterman, 2002). Depolarization can open the voltage-activated Ca^{2+} channels leading to Ca^{2+} influx (Anzai et al., 2000; Wray et al., 2005). Since K^+ channels are the primary regulators of

membrane potentials, inhibition of the K^+ channels results in depolarization and an elevation in intracellular Ca^{2+} (Cook et al., 1988). Since several NADPH oxidases for ROS production are stimulated by elevated intracellular Ca^{2+} (Brandes et al., 2010; Guzik et al., 2008; Hink et al., 2001; Zhang et al., 2008), and since RCS and ROS share the antioxidant detoxification systems, sustained depolarization may augment the production of these reactive species and aggravate oxidative/carbonyl stress.

The adverse effects of MGO on the vasculature have been studied previously. Most of these studies, however, are focused on the molecules of endothelium cells. For example, MGO causes impairment of endothelium-dependent vasorelaxation of rat mesenteric arteries in hyperglycemic conditions by causing dysfunction of the endothelium (Brouwers et al., 2010). MGO stimulates the expression of angiopoietin-2 (Ang-2) protein through the covalent modification of the transcriptional repressor mSin3A causing endothelial cell death in mice (Yao et al., 2007). Our studies indicate that MGO also acts on K^+ channels in VSM cells. The dysfunction of VSM cells is remarkable as the VSMs regulate vascular tones. The disruption of the key proteins in the VSMs for vascular tone regulation tends to impair not only membrane potentials and cellular contractility but also the VSM responses to circulating hormones and neurotransmitters as well as the local factors released by endothelial cells.

Oxidative stress and carbonyl stress have a close relationship. Firstly, previous studies have shown that the elevated levels of MGO can lead to oxidative stress by inactivation of antioxidant enzymes like superoxide dismutase (Desai and Wu, 2008) and glyoxalase (Thornalley, 2003). Secondly, MGO can cause mitochondrial dysfunction leading to uncontrolled production of ROS in VSMs (Wang et al., 2009), which plays a role in the progression of diabetic vascular complications. Thirdly, MGO can promote oxidative stress through AGE receptor (Brownlee,

2001) and the NF-κB signaling pathway to produce ROS (Wu and Juurlink, 2002). Moreover, several antioxidant detoxification systems are shared by RCS and ROS. An over-production of one of the reactive species can compromise the detoxification of the other.

Though MGO can activate the AGE receptor - NF-κB signaling pathway, we feel that this pathway may not be the underlying mechanism for K_{ATP} channel inhibition by MGO for two reasons: 1) Our *in-vitro* assay, in which all the signaling components are missing, shows that MGO can cause mRNA degradation, indicating a direct action rather than an indirect action via signaling pathways. 2) In our previous studies, we have shown that by activating the NF-κB signaling pathway lipopolysaccharides augment, rather than suppress, the expression of vascular K_{ATP} channel mRNAs (Shi et al., 2010).

Our studies suggest that the vascular K_{ATP} channel is indeed inhibited by MGO directly. We have found that an exposure to micromolar concentrations of MGO produces a marked depression of the K_{ATP} currents. Previous studies have shown that plasma MGO levels range from 14.2 μM to 33.6 μM in healthy rats (Wang et al., 2004). Several orders of elevation in the MGO levels are expected to take place in persistent hyperglycemia (Chang and Wu, 2006). The MGO levels may be even higher in local tissues than in the plasma as a result of immediate release from cells. Indeed, the MGO levels are as high as 300 μM when measured in cultured mammalian cells (Chaplen et al., 1998). The concentrations of MGO used for our study are within the physiological range in diabetic conditions.

Our detailed analysis of the mechanisms underlying the decreases in the Kir6.1 and SUR2B transcripts indicates that mRNA instability causes the reduction in the levels of K_{ATP} channel mRNAs. Interestingly, two completely different mechanisms are in action in the process. MGO causes the instability of K_{ATP} channel mRNAs by targeting at the 3'UTR of Kir6.1 gene and

acting directly on the coding region of SUR2B transcripts. To our knowledge, this is the first demonstration of the direct targeting of ion channel mRNA and 3'UTR by MGO.

Because of the intertwining relationship of ROS and RCS, it is necessary to elucidate whether the cellular dysfunction seen in MGO treatment is produced by MGO itself or mediated via the associated oxidative stress. Our current studies support that the mRNAs of Kir6.1 and SUR2B are directly targeted by MGO, while our previous studies have shown that vascular K_{ATP} channel protein is directly targeted in oxidative stress conditions through the post-translational regulation S-glutathionylation (Yang et al., 2011; Yang et al., 2010). Therefore, the data shown in the present studies indicate that MGO has a unique effect on the vascular K_{ATP} channels, though its adverse consequence on channel inhibition is similar to that of oxidative stress. Therefore, carbonyl stress and oxidative stress seem to work synergistically on the vascular K_{ATP} channels. It is likely that the vascular K_{ATP} channels are disrupted in oxidative/carbonyl stress at both protein and mRNA levels, resulting in abnormalities in VMS contractility, dysfunction in vascular responses to circulating/local vasoactive regulators, and exacerbation of oxidative/ carbonyl stress.

REFERENCES

Abramoff, M.D., Magelhaes, P.J., Ram, S.J. (2004). Image Processing with ImageJ. Biophotonics International *11*, 36-42.

Ahmed, N., Argirov, O.K., Minhas, H.S., Cordeiro, C.A., and Thornalley, P.J. (2002). Assay of advanced glycation endproducts (AGEs): surveying AGEs by chromatographic assay with derivatization by 6-aminoquinolyl-N-hydroxysuccinimidyl-carbamate and application to Nepsilon-carboxymethyl-lysine- and Nepsilon-(1-carboxyethyl)lysine-modified albumin. Biochem J *364*, 1-14.

Anzai, K., Ogawa, K., Ozawa, T., and Yamamoto, H. (2000). Oxidative modification of ion channel activity of ryanodine receptor. Antioxid Redox Signal *2*, 35-40.

Asselin, C., Bouchard, B., Tardif, J.C., and Des Rosiers, C. (2006). Circulating 4-hydroxynonenal-protein thioether adducts assessed by gas chromatography-mass spectrometry are increased with disease progression and aging in spontaneously hypertensive rats. Free Radic Biol Med *41*, 97-105.

Baynes, J.W., and Thorpe, S.R. (1999). Role of oxidative stress in diabetic complications: a new perspective on an old paradigm. Diabetes *48*, 1-9.

Bird, M.I., Nunn, P.B., and Lord, L.A. (1984). Formation of glycine and aminoacetone from L-threonine by rat liver mitochondria. Biochim Biophys Acta *802*, 229-236.

Bourajjaj, M., Stehouwer, C.D., van Hinsbergh, V.W., and Schalkwijk, C.G. (2003). Role of methylglyoxal adducts in the development of vascular complications in diabetes mellitus. Biochem Soc Trans *31*, 1400-1402.

Brandes, R.P., Weissmann, N., and Schroder, K. (2010). NADPH oxidases in cardiovascular disease. Free Radic Biol Med *49*, 687-706.

Brennan, C.M., and Steitz, J.A. (2001). HuR and mRNA stability. Cell Mol Life Sci *58*, 266-277.

Brouwers, O., Niessen, P.M., Haenen, G., Miyata, T., Brownlee, M., Stehouwer, C.D., De Mey, J.G., and Schalkwijk, C.G. (2010). Hyperglycaemia-induced impairment of endothelium-dependent vasorelaxation in rat mesenteric arteries is mediated by intracellular methylglyoxal levels in a pathway dependent on oxidative stress. Diabetologia *53*, 989-1000.

Brownlee, M. (1995). Advanced protein glycosylation in diabetes and aging. Annu Rev Med *46*, 223-234.

Brownlee, M. (2001). Biochemistry and molecular cell biology of diabetic complications. Nature *414*, 813-820.

Casazza, J.P., Felver, M.E., and Veech, R.L. (1984). The metabolism of acetone in rat. J Biol Chem *259*, 231-236.

Chang, T., and Wu, L. (2006). Methylglyoxal, oxidative stress, and hypertension. Can J Physiol Pharmacol *84*, 1229-1238.

Chaplen, F.W., Fahl, W.E., and Cameron, D.C. (1998). Evidence of high levels of methylglyoxal in cultured Chinese hamster ovary cells. Proc Natl Acad Sci U S A *95*, 5533-5538.

Chen, C.Y., You, Y., and Shyu, A.B. (1992). Two cellular proteins bind specifically to a purine-rich sequence necessary for the destabilization function of a c-fos protein-coding region determinant of mRNA instability. Mol Cell Biol *12*, 5748-5757.

Chutkow, W.A., Pu, J., Wheeler, M.T., Wada, T., Makielski, J.C., Burant, C.F., and McNally, E.M. (2002). Episodic coronary artery vasospasm and hypertension develop in the absence of Sur2 K(ATP) channels. J Clin Invest *110*, 203-208.

Cook, D.L., Satin, L.S., Ashford, M.L., and Hales, C.N. (1988). ATP-sensitive K+ channels in pancreatic beta-cells. Spare-channel hypothesis. Diabetes *37*, 495-498.

Cooper, K.O., Witz, G., and Witmer, C.M. (1987). Mutagenicity and toxicity studies of several alpha,beta-unsaturated aldehydes in the Salmonella typhimurium mutagenicity assay. Environ Mutagen *9*, 289-295.

Cooper, R.A. (1984). Metabolism of methylglyoxal in microorganisms. Annu Rev Microbiol *38*, 49-68.

Creager, M.A., Luscher, T.F., Cosentino, F., and Beckman, J.A. (2003). Diabetes and vascular disease: pathophysiology, clinical consequences, and medical therapy: Part I. Circulation *108*, 1527-1532.

Department of Health and Human Services, C.f.D.C.a.P. (2011). National diabetes fact sheet: national estimates and general information on diabetes and prediabetes in the United States, 2011. Centers for Disease Control and Prevention *2011*.

Desai, K.M., Chang, T., Wang, H., Banigesh, A., Dhar, A., Liu, J., Untereiner, A., and Wu, L. (2010). Oxidative stress and aging: is methylglyoxal the hidden enemy? Can J Physiol Pharmacol *88*, 273-284.

Desai, K.M., and Wu, L. (2008). Free radical generation by methylglyoxal in tissues. Drug Metabol Drug Interact *23*, 151-173.

Dutra, F., Knudsen, F.S., Curi, D., and Bechara, E.J. (2001). Aerobic oxidation of aminoacetone, a threonine catabolite: iron catalysis and coupled iron release from ferritin. Chem Res Toxicol *14*, 1323-1329.

Ellis, E.M. (2007). Reactive carbonyls and oxidative stress: potential for therapeutic intervention. Pharmacol Ther *115*, 13-24.

Esterbauer, H., Cheeseman, K.H., Dianzani, M.U., Poli, G., and Slater, T.F. (1982). Separation and characterization of the aldehydic products of lipid peroxidation stimulated by ADP-Fe2+ in rat liver microsomes. Biochem J *208*, 129-140.

Esterbauer, H., Schaur, R.J., and Zollner, H. (1991). Chemistry and biochemistry of 4-hydroxynonenal, malonaldehyde and related aldehydes. Free Radic Biol Med *11*, 81-128.

Fan, J., Yang, X., Wang, W., Wood, W.H., 3rd, Becker, K.G., and Gorospe, M. (2002). Global analysis of stress-regulated mRNA turnover by using cDNA arrays. Proc Natl Acad Sci U S A *99*, 10611-10616.

Gutterman, D.D., Miura, H., and Liu, Y. (2005). Redox modulation of vascular tone: focus of potassium channel mechanisms of dilation. Arterioscler Thromb Vasc Biol *25*, 671-678.

Guzik, T.J., Chen, W., Gongora, M.C., Guzik, B., Lob, H.E., Mangalat, D., Hoch, N., Dikalov, S., Rudzinski, P., Kapelak, B., *et al.* (2008). Calcium-dependent NOX5 nicotinamide adenine dinucleotide phosphate oxidase contributes to vascular oxidative stress in human coronary artery disease. J Am Coll Cardiol *52*, 1803-1809.

Hartley, D.P., Ruth, J.A., and Petersen, D.R. (1995). The hepatocellular metabolism of 4-hydroxynonenal by alcohol dehydrogenase, aldehyde dehydrogenase, and glutathione S-transferase. Arch Biochem Biophys *316*, 197-205.

Herring, B.P., El-Mounayri, O., Gallagher, P.J., Yin, F., and Zhou, J. (2006). Regulation of myosin light chain kinase and telokin expression in smooth muscle tissues. Am J Physiol Cell Physiol *291*, C817-827.

Hink, U., Li, H., Mollnau, H., Oelze, M., Matheis, E., Hartmann, M., Skatchkov, M., Thaiss, F., Stahl, R.A., Warnholtz, A., *et al.* (2001). Mechanisms underlying endothelial dysfunction in diabetes mellitus. Circ Res *88*, E14-22.

Kalapos, M.P. (2008). The tandem of free radicals and methylglyoxal. Chem Biol Interact *171*, 251-271.

Krymkiewicz, N. (1973). Reactions of methylglyoxal with nucleic acids. FEBS Lett *29*, 51-54.

Kuhla, B., Luth, H.J., Haferburg, D., Boeck, K., Arendt, T., and Munch, G. (2005). Methylglyoxal, glyoxal, and their detoxification in Alzheimer's disease. Ann N Y Acad Sci *1043*, 211-216.

Leonarduzzi, G., Chiarpotto, E., Biasi, F., and Poli, G. (2005). 4-Hydroxynonenal and cholesterol oxidation products in atherosclerosis. Mol Nutr Food Res *49*, 1044-1049.

Lesgards, J.F., Gauthier, C., Iovanna, J., Vidal, N., Dolla, A., and Stocker, P. (2011). Effect of reactive oxygen and carbonyl species on crucial cellular antioxidant enzymes. Chem Biol Interact *190*, 28-34.

Liu, Y., and Gutterman, D.D. (2002). Oxidative stress and potassium channel function. Clin Exp Pharmacol Physiol *29*, 305-311.

Liu, Y., and Gutterman, D.D. (2009). Vascular control in humans: focus on the coronary microcirculation. Basic Research in Cardiology *104*, 211-227.

Lo, C.Y., Li, S., Tan, D., Pan, M.H., Sang, S., and Ho, C.T. (2006). Trapping reactions of reactive carbonyl species with tea polyphenols in simulated physiological conditions. Mol Nutr Food Res *50*, 1118-1128.

Lo, T.W., Westwood, M.E., McLellan, A.C., Selwood, T., and Thornalley, P.J. (1994). Binding and modification of proteins by methylglyoxal under physiological conditions. A kinetic and mechanistic study with N alpha-acetylarginine, N alpha-acetylcysteine, and N alpha-acetyllysine, and bovine serum albumin. J Biol Chem *269*, 32299-32305.

Lovell, M.A., Xie, C., and Markesbery, W.R. (2001). Acrolein is increased in Alzheimer's disease brain and is toxic to primary hippocampal cultures. Neurobiol Aging *22*, 187-194.

Lyles, G.A., and Chalmers, J. (1992). The metabolism of aminoacetone to methylglyoxal by semicarbazide-sensitive amine oxidase in human umbilical artery. Biochem Pharmacol *43*, 1409-1414.

Marnett, L.J., Hurd, H.K., Hollstein, M.C., Levin, D.E., Esterbauer, H., and Ames, B.N. (1985). Naturally occurring carbonyl compounds are mutagens in Salmonella tester strain TA104. Mutat Res *148*, 25-34.

McLellan, A.C., Thornalley, P.J., Benn, J., and Sonksen, P.H. (1994). Glyoxalase system in clinical diabetes mellitus and correlation with diabetic complications. Clin Sci (Lond) *87*, 21-29.

Miki, T., Suzuki, M., Shibasaki, T., Uemura, H., Sato, T., Yamaguchi, K., Koseki, H., Iwanaga, T., Nakaya, H., and Seino, S. (2002). Mouse model of Prinzmetal angina by disruption of the inward rectifier Kir6.1. Nat Med *8*, 466-472.

Miura, H., Wachtel, R.E., Loberiza, F.R., Jr., Saito, T., Miura, M., Nicolosi, A.C., and Gutterman, D.D. (2003). Diabetes mellitus impairs vasodilation to hypoxia in human coronary arterioles: reduced activity of ATP-sensitive potassium channels. Circ Res *92*, 151-158.

Nukaya, H., Inaoka, Y., Ishida, H., Tsuji, K., Suwa, Y., Wakabayashi, K., and Kosuge, T. (1993). Modification of the amino group of guanosine by methylglyoxal and other alpha-ketoaldehydes in the presence of hydrogen peroxide. Chem Pharm Bull (Tokyo) *41*, 649-653.

Ohsawa, I., Nishimaki, K., Yasuda, C., Kamino, K., and Ohta, S. (2003). Deficiency in a mitochondrial aldehyde dehydrogenase increases vulnerability to oxidative stress in PC12 cells. J Neurochem *84*, 1110-1117.

Papoulis, A., al-Abed, Y., and Bucala, R. (1995). Identification of N2-(1-carboxyethyl)guanine (CEG) as a guanine advanced glycosylation end product. Biochemistry *34*, 648-655.

Picklo, M.J., Montine, T.J., Amarnath, V., and Neely, M.D. (2002). Carbonyl toxicology and Alzheimer's disease. Toxicol Appl Pharmacol *184*, 187-197.

Pompliano, D.L., Peyman, A., and Knowles, J.R. (1990). Stabilization of a reaction intermediate as a catalytic device: definition of the functional role of the flexible loop in triosephosphate isomerase. Biochemistry *29*, 3186-3194.

Rosca, M.G., Mustata, T.G., Kinter, M.T., Ozdemir, A.M., Kern, T.S., Szweda, L.I., Brownlee, M., Monnier, V.M., and Weiss, M.F. (2005). Glycation of mitochondrial proteins from diabetic rat kidney is associated with excess superoxide formation. Am J Physiol Renal Physiol *289*, F420-430.

Ross, J. (1995). mRNA stability in mammalian cells. Microbiol Rev *59*, 423-450.

Sachs, A.B. (1993). Messenger RNA degradation in eukaryotes. Cell *74*, 413-421.

Sato, J., Wang, Y.M., and van Eys, J. (1980). Methylglyoxal formation in rat liver cells. J Biol Chem *255*, 2046-2050.

Schmidt, A.M., Yan, S.D., Wautier, J.L., and Stern, D. (1999). Activation of receptor for advanced glycation end products: a mechanism for chronic vascular dysfunction in diabetic vasculopathy and atherosclerosis. Circ Res *84*, 489-497.

Schneider, M., Quistad, G.B., and Casida, J.E. (1998). N2,7-bis(1-hydroxy-2-oxopropyl)-2'-deoxyguanosine: identical noncyclic adducts with 1,3-dichloropropene epoxides and methylglyoxal. Chem Res Toxicol *11*, 1536-1542.

Shi, W., Cui, N., Wu, Z., Yang, Y., Zhang, S., Gai, H., Zhu, D., and Jiang, C. (2010). Lipopolysaccharides up-regulate Kir6.1/SUR2B channel expression and enhance vascular KATP channel activity via NF-kappaB-dependent signaling. J Biol Chem *285*, 3021-3029.

Shipanova, I.N., Glomb, M.A., and Nagaraj, R.H. (1997). Protein modification by methylglyoxal: chemical nature and synthetic mechanism of a major fluorescent adduct. Arch Biochem Biophys *344*, 29-36.

Shyu, A.B., Belasco, J.G., and Greenberg, M.E. (1991). Two distinct destabilizing elements in the c-fos message trigger deadenylation as a first step in rapid mRNA decay. Genes Dev *5*, 221-231.

Thornalley, P.J. (1990). The glyoxalase system: new developments towards functional characterization of a metabolic pathway fundamental to biological life. Biochem J *269*, 1-11.

Thornalley, P.J. (1998). Cell activation by glycated proteins. AGE receptors, receptor recognition factors and functional classification of AGEs. Cell Mol Biol (Noisy-le-grand) *44*, 1013-1023.

Thornalley, P.J. (2003). Glyoxalase I--structure, function and a critical role in the enzymatic defence against glycation. Biochem Soc Trans *31*, 1343-1348.

Thornalley, P.J. (2005). Dicarbonyl intermediates in the maillard reaction. Ann N Y Acad Sci *1043*, 111-117.

Thornalley, P.J., Battah, S., Ahmed, N., Karachalias, N., Agalou, S., Babaei-Jadidi, R., and Dawnay, A. (2003). Quantitative screening of advanced glycation endproducts in cellular and extracellular proteins by tandem mass spectrometry. Biochem J *375*, 581-592.

Thornalley, P.J., Langborg, A., and Minhas, H.S. (1999). Formation of glyoxal, methylglyoxal and 3-deoxyglucosone in the glycation of proteins by glucose. Biochem J *344 Pt 1*, 109-116.

Vaca, C.E., Fang, J.L., Conradi, M., and Hou, S.M. (1994). Development of a 32P-postlabelling method for the analysis of 2'-deoxyguanosine-3'-monophosphate and DNA adducts of methylglyoxal. Carcinogenesis *15*, 1887-1894.

Vander Jagt, D.L., Hunsaker, L.A., Vander Jagt, T.J., Gomez, M.S., Gonzales, D.M., Deck, L.M., and Royer, R.E. (1997). Inactivation of glutathione reductase by 4-hydroxynonenal and other endogenous aldehydes. Biochem Pharmacol *53*, 1133-1140.

Vander Jagt, D.L., Robinson, B., Taylor, K.K., and Hunsaker, L.A. (1992). Reduction of trioses by NADPH-dependent aldo-keto reductases. Aldose reductase, methylglyoxal, and diabetic complications. J Biol Chem *267*, 4364-4369.

Vasdev, S., Ford, C.A., Longerich, L., Gadag, V., and Wadhawan, S. (1998). Role of aldehydes in fructose induced hypertension. Mol Cell Biochem *181*, 1-9.

Vasiliou, V., Pappa, A., and Estey, T. (2004). Role of human aldehyde dehydrogenases in endobiotic and xenobiotic metabolism. Drug Metab Rev *36*, 279-299.

Vlassara, H. (1996). Advanced glycation end-products and atherosclerosis. Ann Med *28*, 419-426.

Wang, H., Liu, J., and Wu, L. (2009). Methylglyoxal-induced mitochondrial dysfunction in vascular smooth muscle cells. Biochem Pharmacol *77*, 1709-1716.

Wang, X., Desai, K., Clausen, J.T., and Wu, L. (2004). Increased methylglyoxal and advanced glycation end products in kidney from spontaneously hypertensive rats. Kidney Int *66*, 2315-2321.

Wautier, J.L., and Schmidt, A.M. (2004). Protein glycation: a firm link to endothelial cell dysfunction. Circ Res *95*, 233-238.

Webb, R.C. (2003). Smooth muscle contraction and relaxation. Adv Physiol Educ *27*, 201-206.

Wray, S., Burdyga, T., and Noble, K. (2005). Calcium signalling in smooth muscle. Cell Calcium *38*, 397-407.

Wu, L. (2006). Is methylglyoxal a causative factor for hypertension development? Can J Physiol Pharmacol *84*, 129-139.

Wu, L., and Juurlink, B.H. (2002). Increased methylglyoxal and oxidative stress in hypertensive rat vascular smooth muscle cells. Hypertension *39*, 809-814.

Yang, Y., Shi, W., Chen, X., Cui, N., Konduru, A.S., Shi, Y., Trower, T.C., Zhang, S., and Jiang, C. (2011). Molecular basis and structural insight of vascular K(ATP) channel gating by S-glutathionylation. J Biol Chem *286*, 9298-9307.

Yang, Y., Shi, W., Cui, N., Wu, Z., and Jiang, C. (2010). Oxidative stress inhibits vascular K(ATP) channels by S-glutathionylation. J Biol Chem *285*, 38641-38648.

Yang, Y., Shi, Y., Guo, S., Zhang, S., Cui, N., Shi, W., Zhu, D., and Jiang, C. (2008). PKA-dependent activation of the vascular smooth muscle isoform of KATP channels by vasoactive intestinal polypeptide and its effect on relaxation of the mesenteric resistance artery. Biochim Biophys Acta *1778*, 88-96.

Yao, D., Taguchi, T., Matsumura, T., Pestell, R., Edelstein, D., Giardino, I., Suske, G., Rabbani, N., Thornalley, P.J., Sarthy, V.P., *et al.* (2007). High glucose increases angiopoietin-2 transcription in microvascular endothelial cells through methylglyoxal modification of mSin3A. J Biol Chem *282*, 31038-31045.

Zhang, F., Jin, S., Yi, F., Xia, M., Dewey, W.L., and Li, P.L. (2008). Local production of O2- by NAD(P)H oxidase in the sarcoplasmic reticulum of coronary arterial myocytes: cADPR-mediated Ca2+ regulation. Cell Signal *20*, 637-644.